MODERN PATHOLOGY

ABSTRACTS

PULMONARY, MEDIASTINAL, PLEURAL, AND PERITONEAL PATHOLOGY
(910-952)

USCAP 110TH ANNUAL MEETING

NEVER STOP
LEARNING
2021

MARCH 13-18, 2021 | VIRTUAL AND INTERACTIVE

To cite abstracts in this publication, please use the following format: **Author A, Author B, Author C, et al. Abstract title (abs#). In "File Title."** *Modern Pathology* **2021; 34 (suppl 2): page#**

910 Relevance of Next-Generation Sequencing in Non-Small Cell Lung Cancer; Molecular Epidemiology Study in Indian Patients

Aditi Aggarwal[1], Neha Sabnis[1], Avshesh Mishra[2], Vipin Kumar[2], Sagar Samrat Mohanty[2], Lata Kini[1], Shivani Sharma[1], Sambit Mohanty[3]
[1]Core Diagnostics, Gurgaon, India, [2]Core Diagnostics, Gurugram, India, [3]AMRI Hospital, Chandigarh, India

Disclosures: Aditi Aggarwal: None; Neha Sabnis: None; Avshesh Mishra: None; Vipin Kumar: None; Sagar Samrat Mohanty: None; Lata Kini: None; Shivani Sharma: None; Sambit Mohanty: None

Background: The understanding of molecular mechanisms involved in the non-small cell lung carcinoma (NSCLC) has increased significantly in the recent years. These have helped to develop personalized management strategies by identifying specific molecular alterations such as mutations in EGFR, ROS1, BRAF, ERBB2, MET, ALK, and KRAS genes. These mutations are targetable by various therapeutic molecules, ensuring a better clinical outcome. Next generation sequencing (NGS) methodology is the recommended technique for the identification of driver mutations in the five hot-spot genes (EGFR, ALK, ROS1, MET, and BRAF) involved in the NSCLC carcinogenesis. NGS has numerous advantages (multiplexing, tissue conservation, identification of rare and novel variants, and reduced cost and combined turn-around time) over sequential single gene testing. Herein, we demonstrate the molecular mutational profiling and their clinicopathologic correlation in a large cohort of Indian NSCLC cancer patients.

Design: Five fifty two Stage IV NSCLC patients (n=552; adenocarcinoma, n=490; squamous cell carcinoma, n=51; adenosquamous carcinoma, n=5; large cell carcinoma, n=2; sarcomatoid carcinoma, n=3; spindle cell carcinoma, n=1) underwent broad molecular profiling by a custom-made, targeted DNA- and RNA-based five hot-spot genes lung cancer panel (EGFR, ALK, ROS1, BRAF and MET), compatible with the NGS Ion S5 system. The mutations were correlated with the clinicopathologic characteristics.

Results: Validation of the 5 gene panel yielded the following results: a) Specificity of 99.74%; b) Sensitivity of 100% for SNVs (>5% VAF), Indels (>10% VAF) and fusions; c) 100% intra- and inter-run reproducibility; d) 88% inter-laboratory agreement. Validated panel was then used to analyze clinical samples. 320 of 552 (57.97%) tumors (patients) harbored either one (302 or 54.71%) or multiple (18 or 3.26%) mutations. EGFR and BRAF V600E mutations, ALK and ROS1 rearrangements, and MET exon 14 skipping mutation were observed in in 38.41% and 2.72% patients, 12.14% and 3.62% patients, and 1.09% patients. EGFR exon 19 deletions accounted for 52.83% of all mutations, followed by L858R (35.85%), T790M (5.19%), exon 20 insertions (6.60%) and other rare mutations (G719X, L861Q, S768I) (9.91%). Concurrent EGFR with ALK, EGFR with ROS1, EGFR with MET and EGFR with BRAF were observed in 10, 4, 1, and 3 patients.

Total Positive Cases		EGFR (n=212)	ALK (n=67)	ROS (n-20)	MET (n=6)	BRAF (n=15)
Gender	Female	104 (49.06%)	28 (41.8%)	9 (45%)	3 (50%)	8 (53.34%)
	Male	108 (50.95%)	39 (58.21%)	11 (55%)	3 (50%)	7 (46.67%)
Age	less than 30yrs	1 (0.48%)	4 (5.98%)	1 (5%)	0(0 %)	0(0 %)
	31-60 years	107 (50.48%)	42 (62.69%)	11 (55%)	2 (33.34%)	7 (46.67%)
	more than 60 years	104 (49.06%)	21 (31.35%)	8 (40%)	4 (66.67%)	8 (53.34%)
Smoking Status	Smoker Females	9(4.25 %)	1(1.5 %)	0(0 %)	0(0 %)	2(13.34 %)
	Smoker Males	32(15.1 %)	3(4.48 %)	5(25 %)	1(16.67 %)	4(26.67 %)
	Non-Smoker Females	75(35.38 %)	21(31.35 %)	9(45 %)	3(50 %)	5(33.34 %)
	Non-Smoker Males	59(27.84 %)	29(43.29 %)	5(25 %)	1(16.67 %)	3(20 %)
	Unknown smoking status Females	15(7.08 %)	6(8.96 %)	0(0 %)	0(0 %)	1(16.67 %)
	Unknown smoking status Males	11(5.19 %)	1(1.5 %)	1(5 %)	1(16.67 %)	0(0 %)

Tissue for NGS	Primary site	133 (62.74%)	39 (58.21%)	11 (55%)	2 (33.34%)	8 (53.34%)
	Metastatic site	79 (37.27%)	28 (41.8%)	9 (45%)	4 (66.67%)	7 (46.67%)
Histologic Type	Adenocarcinoma	197 (92.92%)	65 (97%)	18 (90%)	5 (83.33%)	13 (86.67%)
	Squamous Cell Carcinoma	11 (5.19%)	2 (2.99%)	1 (5%)	1 (16.67%)	1 (6.67%)
	Adenosquamous Carcinoma	3 (1.42%)	0 (0%)	0 (0%)	0 (0%)	0 (0%)
	Large Cell Carcinoma	1 (0.48%)	0 (0%)	0 (0%)	0 (0%)	0 (0%)
	Sarcomatoid Carcinoma	0 (0%)	0 (0%)	1 (5%)	0 (0%)	0 (6.67%)

Figure 1 - 910

Correlation between various histologic types and mutational profiles.
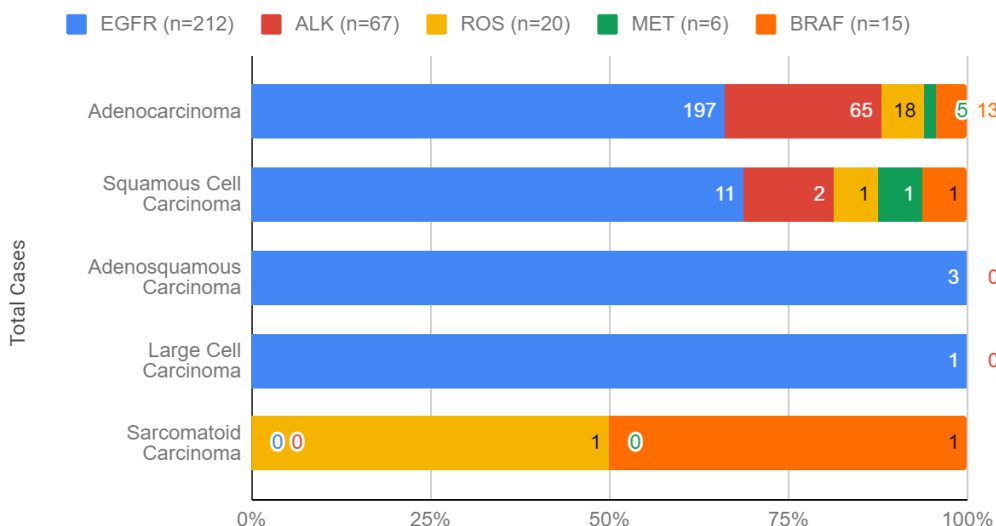
1. This is the largest cohort of NSCLC for comprehensive targeted mutational profiling.
2. The mutations are more prevalent in non-smoker females for all genes except ALK (non-smoker males).
3. MET and BRAF mutations are more common in elderly population whereas EGFR mutations, and ALK and ROS1 genes rearrangements are more prevalent in younger population.
4. The most common histopathologic subtype associated with various mutations are as follows: acinar with EGFR, solid with ALK, macronucleoli with ROS1, signet ring with MET, and micropapillary with BRAF (Figure 1 and 2).

911 Unacceptable Donor Lungs Before and After Ex Vivo Lung Perfusion: A Focus on Histologic Spectrum

Amandeep Aneja[1], Anu Peter[1], Abul Kashem[1], Nirag Jhala[1], Yoshiya Toyoda[1]
[1]Temple University Hospital, Philadelphia, PA

Disclosures: Amandeep Aneja: None; Anu Peter: None; Abul Kashem: None; Nirag Jhala: None; Yoshiya Toyoda: None

Background: Ex-vivo lung perfusion (EVLP), is an innovative technique applied to donor lungs that could provide platform to preserve, evaluate, and repair the donor lung graft. EVLP improves organ quality making previously unsuitable lungs safe for transplant. We report our experience of histologic assessment of before and after EVLP in tissue samples from discarded human lungs.

Design: Lungs from 16 brain-dead donors from four different institutes were enrolled in the study. After harvesting, the lungs were stored at 4°C for 10 hours and subjected to normothermic EVLP with Steen Solution for a duration ranging between minimum of 6 hours up to a maximum of 12 hours. Each lung was biopsied at 4 different time intervals: before perfusion, 1 hour, 4 hour and end of study (EOS). Two pathologists assessed the histopathologic grading of acute lung injury (ALI) using the parameters of alveolar injury, interstitial and vascular changes, apoptosis and necrosis. A 4-point scale as 0, absent; 1, mild; 2, moderate; and 3, severe was used to grade the findings. The sum of each parameter resulted in the Lung Injury Score (LIS). Detection of apoptosis through terminal deoxynucleotidyl transferase dUTP nick end labeling (TUNEL) and anti-active caspase-3 antibody was undertaken.

Results: All 16 lungs showed maintained lung tissue structure during the process of perfusion and EOS. 14 lungs showed a decrease in LIS score at EOS, the reduction ranging between 1-5 points. No significant difference in LIS was noted in remaining two lungs. Alveolar changes showed a general trend towards reduction in the intra-alveolar edema, hemorrhage, and fibrin deposition over the four different time points of evaluation moving towards EOS whereas, interstitial changes (cellular infiltration, interstitial widening, and capillary congestion) showed a mild decrease to no significant change. Apoptosis was evaluated by randomly choosing 5 fields/slide. Minimal apoptosis was noted in six out of sixteen lungs, out of which only one lung revealed apoptosis at EOS. The minimal decrease noted in the interstitium may be related to the expected hemodynamic changes secondary to perfusion. Moreover, no significant apoptotic activity indicated cell death cascade was most likely not activated. Vascular integrity was not compromised before the start of the perfusion and showed no change throughout the process.

Conclusions: EVLP decreases LIS and therefore offers string potential to increase organ availability for selected patients in need.

912 PD-L1 Expression and CD8 Positive T Cell Tumor Infiltrate Level Predict Response to Immune Checkpoint Inhibitors in Non-Small Cell Lung Cancer

Manuel Arana Rosainz[1], Matthew Gayhart[1], Manita Chaum[2], Celeste Eno[1], Jianbo Song[1], Fabiola Medeiros[1], Eric Vail[1], Jean Lopategui[2]
[1]Cedars-Sinai Medical Center, Los Angeles, CA, [2]Cedars-Sinai Medical Center, West Hollywood, CA

Disclosures: Manuel Arana Rosainz: None; Matthew Gayhart: None; Manita Chaum: None; Celeste Eno: None; Jianbo Song: None; Fabiola Medeiros: None; Eric Vail: None; Jean Lopategui: None

Background: Cancer immunotherapy, especially immune checkpoint inhibitors (ICIs), can have a remarkable antitumor response in non-small cell lung cancer (NSCLC). However, the majority of patients fail to respond to PD-1/PD-L1 axis inhibitors. Pembrolizumab is indicated as a first-line therapy for patients with advanced NSCLC with PD-L1 expression Tumor Proportion Score (TPS) >1%. Although expression of PD-L1 and tumor environment immune cells have been independently associated with response rates, the contribution of these factors for better prediction of the response to ICI therapy in NSCLC is still largely unclear. In a previous small pilot study, we observed that both high PD-L1 expression and the percentage and pattern of CD4/8 positive T-cells appear to be better predictive of ICI response in NSCLC than PD-L1 alone. Herein we further evaluate the predictive value of these biomarkers by using a more extensive study sample set.

Design: A total of 26 NSCLC patients who received ICIs (8 responders and 18 non-responders) were identified from the departmental surgical pathology archives and response data was retrieved from the electronic medical record. Responders were defined as those achieving at least a partial response (30% decrease or more in the sum of diameters of target lesions) according to RECIST guideline v1.1. Response was assessed at 6-8 weeks after ICI therapy initiation with follow-up of at least 6 months. Immunohistochemistry (IHC) studies for PD-L1, CD4, CD8, CD21, and CD163 were performed and the results were tabulated. High PD-L1 expression was defined as TPS>50%; immune cell tumor infiltrate level was classified as high (>10%) or low (<5%).

Results: In our study, non-responders mostly displayed low PD-L1 expression (mean TPS: 19.8%; range 1-70%) and low or no CD8 positive T-cell tumor infiltrate (13/18; 72.2%). In contrast, most responders displayed a high PD-L1 expression (mean TPS: 55.5%; range 1-100%) with most (7/8, 87.5%) having a high CD8 positive T-cell tumor

infiltrate. The level of tumor infiltrating CD4 positive T-cells and CD163 positive macrophages was similar for both groups. No CD21 positive cells infiltrating tumor were identified in any of the specimens.

Conclusions: Our study highlights the current dilemma in treating NSCLC with ICIs as over two-thirds of our patients did not respond to treatment. However, a combination of high PD-L1 expression and high CD8 expression is much more accurate in determining response to ICI therapy and should be routinely assessed to assist in predicting response. Prospective study is underway to confirm the predictive value of these combined biomarkers.

913 Tuft Cell Master Regulator POU2F3 is a Novel Helpful Diagnostic Immunohistochemical Marker in Neuroendocrine-Low Small Cell Lung Carcinomas

Marina Baine[1], Min-Shu Hsieh[2], Wei-Chu Lai[1], Jacklynn Egger[1], Achim Jungbluth[1], Jennifer Sauter[1], Jason Chang[1], Darren Buonocore[1], William Travis[1], Triparna Sen[1], John Poirier[3], Charles Rudin[1], Robert Homer[4], Natasha Rekhtman[1]
[1]Memorial Sloan Kettering Cancer Center, New York, NY, [2]National Taiwan University Hospital, Taipei, Taiwan, [3]NYU Langone School of Medicine, New York, NY, [4]Yale School of Medicine, New Haven, CT

Disclosures: Marina Baine: None; Min-Shu Hsieh: None; Wei-Chu Lai: None; Jacklynn Egger: None; Achim Jungbluth: None; Jennifer Sauter: None; Jason Chang: None; Darren Buonocore: None; William Travis: None; Triparna Sen: None; John Poirier: None; Charles Rudin: *Consultant*, Amgen; *Consultant*, AstraZeneca; *Consultant*, Roche; *Consultant*, Ipsen; *Consultant*, Jazz; Robert Homer: None; Natasha Rekhtman: None

Background: A minority of small cell lung carcinomas (SCLC) has minimal or absent expression of neuroendocrine (NE) markers, which can present a diagnostic challenge. Recent studies have suggested that POU2F3 – a marker of chemosensory tuft cell lineage – is expressed specifically in NE-low SCLC. Here, we aimed to examine expression of POU2F3 in SCLC with extremely low or negative NE markers and to determine its specificity relative to non-NE lung carcinomas.

Design: POU2F3 expression was examined immunohistochemically in 152 SCLC and 116 non-small cell lung carcinomas (NSCLC; 53 adenocarcinomas, 63 squamous cell carcinomas). SCLC comprised 144 unselected cases and 8 additional pre-selected NE-minimal or negative SCLC. All SCLC were tested for 4 conventional NE markers (CNM; synaptophysin, chromogranin, CD56, and INSM1), and tumors with combined NE score (average H-score of 4 CNM) <50 were defined as NE-low and those with score <10 (staining isolated cells only) as NE-minimal. TTF-1 expression was also evaluated.

Results: POU2F3 was expressed in 8% of unselected SCLC (11/140), but was completely negative in all 116 NSCLC. In the whole cohort, compared to POU2F3-negative cases (n=134), POU2F3-positive SCLC (n=18) had fewer positive CNM (mean 1.8 vs 3.7, p<0.0001), lower combined NE score (mean 60 vs 183, p<0.0001) and lower rate of TTF-1 expression (6% vs 81%, p<0.0001), respectively. A total of 15 SCLC were NE-low (n=10), NE-minimal (n=4) or NE-entirely negative (n=1). POU2F3 was positive in 10/15 (67%) of these cases, including all 5 NE-minimal/negative SCLC. POU2F3 expression in these cases was typically strong and diffuse (mean H-score 147; range 60-235).

Conclusions: POU2F3 expression is highly specific for SCLC relative to NSCLC, and is significantly enriched in NE-low SCLC, particularly in cases with minimal or negative NE marker expression. We suggest that POU2F3 represents a novel helpful diagnostic marker of SCLC.

914 The Utility of Secretagogin as a Novel Marker for the Diagnosis of Lung Neuroendocrine Carcinoma

Yigit Baykara[1], Ying Xiao[1], Dongfang Yang[2], Evgeny Yakirevich[2], Maria Garcia-Moliner[2], Li Juan Wang[1], Shaolei Lu[1]
[1]Alpert Medical School of Brown University, Providence, RI, [2]Rhode Island Hospital, Providence, RI

Disclosures: Yigit Baykara: None; Ying Xiao: None; Dongfang Yang: None; Evgeny Yakirevich: None; Li Juan Wang: None; Shaolei Lu: None

Background: Synaptophysin, Chromogranin A, and CD56 are established neuroendocrine (NE) markers for lung neuroendocrine carcinomas (NECs). However, none of these markers are perfectly sensitive or specific, there is a need for alternative markers to improve diagnosis. In our study, we examined the utility of a novel neuroendocrine marker secretagogin (SCGN) for diagnosing lung neuroendocrine carcinomas. SCGN is a calcium-binding secretory/cytoplasmic protein that is encoded by the SCGN gene and acts as a calcium sensor. SCGN is expressed exclusively in neurons, neuroblasts and neuroendocrine cells, and its deficiency is thought to play an important role in several endocrinologic and neurologic disorders.

Design: The study included 46 resections, including 12 small cell carcinomas (SCCs), 15 large cell carcinomas (LCCs), 9 combined small and large cell carcinomas (CSLCs), and 10 combined large cell carcinoma and adenocarcinomas (CLCCAs) from the pathology archive from 2012-2018. Immunohistochemical stainings with SCGN were done along with synaptophysin, chromogranin A and CD56. The stainings were evaluated for both the staining intensity and proportion of the stained cells to the total number of cancer cells on the slide. The positive stain was defined as at least mild staining intensity in at least 1% of the tumor cells. The mean intensity score and the mean proportion of the stained cells of SCGN were compared to the mean intensity scores and the mean proportion of the stained cells of other markers using a paired T-test.

Results: Synaptophysin showed exclusively diffuse cytoplasmic staining in neuroendocrine cells (Figures 1 and 2) and was positive in 85% (39/46), Chromogranin A in 57% (26/46), CD56 in 89% (31/35), and SCGN in 59% (27/46) of NECs. SCGN expression was significantly more abundant in NEC than chromogranin A (P=0.0347). SCGN was positive in 0 of 7 synaptophysin-negative, 5 of 20 chromogranin A-negative, and 2 of 17 CD56-negative tumors. 94% of NECs were positive for either CD56 or SCGN; 67% of NECs were positive for either Chromogranin A or SCGN; 96% of NECs were positive for either CD56, Chromogranin A, or SCGN. 11 of 12 (92%) SCCs were positive for SCGN, in compared to 2 of 12 (17%) for Chromogranin A.

Figure 1 - 914

SCGN stain 200x
Small cell carcinoma

Figure 2 - 914

SCGN stain 200x
Large cell carcinoma
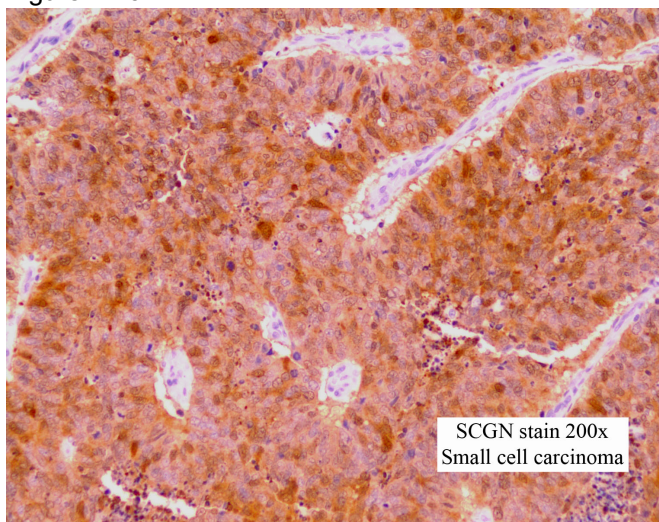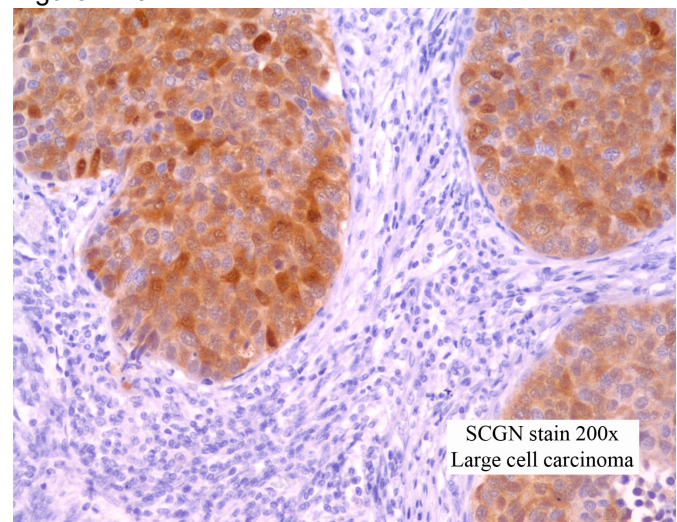
Conclusions: The combined use of multiple neuroendocrine markers helps to increase diagnostic sensitivity and specificity. SCGN was positive in 59% of NECs and can be used as an additional neuroendocrine marker to diagnose NECs. SCGN can be expressed in NECs negative for chromogranin A, and CD 56. Its expression in NECs was more robust than chromogranin A. Its positive rate in small cell carcinomas (92%) is higher than chromogranin A (17%).

915   Pulmonary Capillaritis as a Manifestation of Checkpoint Inhibitor Pulmonary Toxicity

Leyla Canbeldek[1], Allen Burke[2]
[1]University of Maryland Medical Center, Baltimore, MD, [2]University of Maryland Medical School of Medicine, Baltimore, MD

Disclosures: Leyla Canbeldek: None; Allen Burke: None

Background: Checkpoint inhibitor therapy is a known cause of lung toxicity. There have been few histologic descriptions of pathologic features of pneumonitis clinically attributed to checkpoint inhibitor therapy, and vasculitis has not yet been reported in this setting.

Design: We report histologic findings of biopsies of 3 patients who developed pulmonary symptoms that were temporally associated with monoclonal antibody treatment. Clinical information and radiologic findings were obtained by chart review.

Results: Three patients (2 male; 1 female; age range 20-72 years) with history of malignancy presented with pulmonary symptoms and showed CT findings of bilateral ground glass opacities. All patients were being treated with Pembrolizumab or Nivolumumab for at least one month. No patient had diffuse alveolar hemorrhage. Clinical diagnosis of presumed drug toxicity made after infectious etiologies ruled out. All cases showed interstitial neutrophilic inflammation, two with prominent capillary involvement. Follow up histories showed resolution of symptoms after cessation of the checkpoint inhibitor therapy. (Table 1)

Age/Sex	20y/M	48y/F	72y/M
Treatment / duration	Pembrolizumab / 19 months	Nivolumab/ 39 months	Nivolumab/ 1 month
Malignancy	Metastatic EBV associated nasopharyngeal carcinoma	Nodular sclerosis Hodgkin's lymphoma	Diffuse malignant mesothelioma, pleura
Clinical Symptoms	Shortness of breath	Cough for over 3 weeks	Productive cough, diffuse pruritic skin rash
Radiology (CT)	Ground glass opacities	Ground glass changes	Ground glass opacities
Pathology	Interstitial infiltrate with neutrophils, apoptotic debris, mononuclear inflammation. Diffuse pneumocyte hyperplasia and focal fibrin exudate in airspaces	Interstitial inflammation with neutrophils, apoptotic bodies, and patchy organizing alveolar injury	Interstitial inflammation with neutrophils, apoptotic bodies, eosinophils, mononuclear inflammation Focal acute bronchiolitis Focal acute alveolar injury

Figure 1 - 915
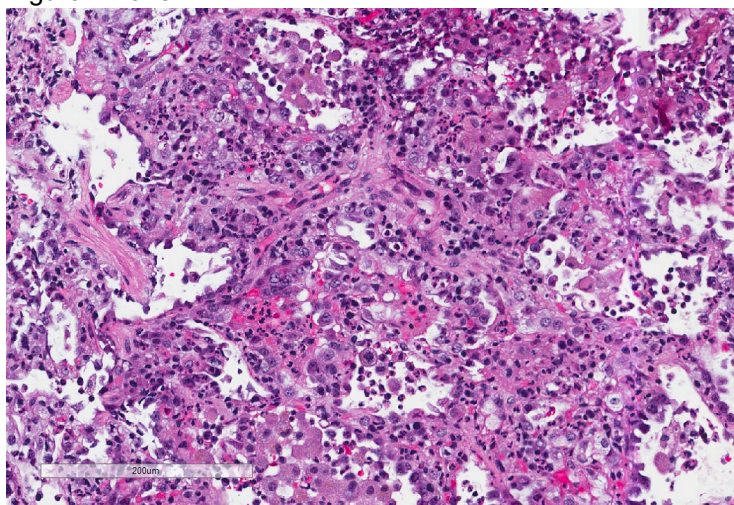
Conclusions: Capillaritis without diffuse alveolar hemorrhage may be a manifestation of checkpoint inhibitor toxicity.

916   Application of NF2 Immunohistochemistry for the Diagnosis of Mesothelioma

Mariana Canepa[1], Sara Maleki[2], Evgeny Yakirevich[3]
[1]Alpert Medical School of Brown University, Providence, RI, [2]Brown University, Rhode Island Hospital, Providence, RI, [3]Rhode Island Hospital, Providence, RI

Disclosures: Mariana Canepa: None; Sara Maleki: None; Evgeny Yakirevich: None

Background: Distinction between mesothelial hyperplasia and mesothelioma is essential once a proliferation is proven to be mesothelial in origin. The use of small samples obtained by minimally invasive methods for first-time diagnosis is common given physical condition limitations in these patients. However, morphologic criteria for mesothelioma such as invasion of the fat are not always present in biopsy specimens. It has been suggested in animal models that disruption of the NF2 signalling is essential for the development of human mesothelioma either by *NF2* gene mutation or NF2/Merlin protein inactivation by phosphorylation. We aimed to evaluate NF2 inactivation by immunohistochemistry (IHC) in cases of mesothelioma.

Design: We searched our institutional archives between 2010-2020 to identify 11 mesothelioma cases. For comparison, seven cases with normal mesothelial lining or reactive mesothelial hyperplasia were included. The NF2 IHC was performed with D3S3W monoclonal antibody from Cell Signalling Technology in 1:100 dilution. In five cases MTAP (clone 2G4 from Abnova) and BAP1 (clone C-4 from Santa Cruz Biotechnology Inc.) IHC was done at an outside institution.

Results: In all seven cases with normal mesothelial lining or reactive mesothelial hyperplasia NF2 demonstrated membranous immunoreactivity of mesothelial cells (Figure 1). The eleven mesothelioma cases consisted of seven pleural biopsies, three pleural resections and a total omentectomy. The patients were 7 males and 3 females between the ages of 43 and 84 years old. The majority were epithelioid type (seven), with three sarcomatoid and one biphasic mesothelioma. Nine of eleven cases (82%) including the sarcomatoid and biphasic demonstrated loss of NF2 staining (Figure 2). Two of the epithelioid pleural mesotheliomas (18%) showed preserved NF2 staining. NF2 loss was useful in five cases where preserved BAP1 and MTAP expression could not prove the diagnosis of mesothelioma.
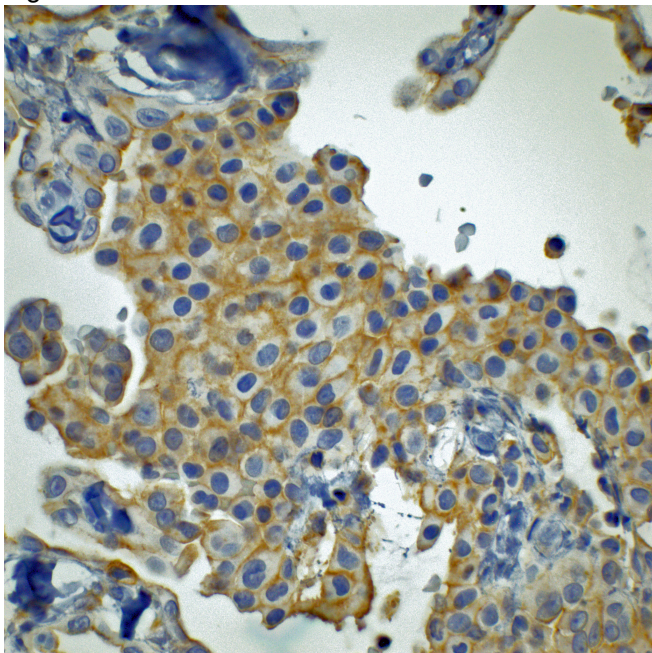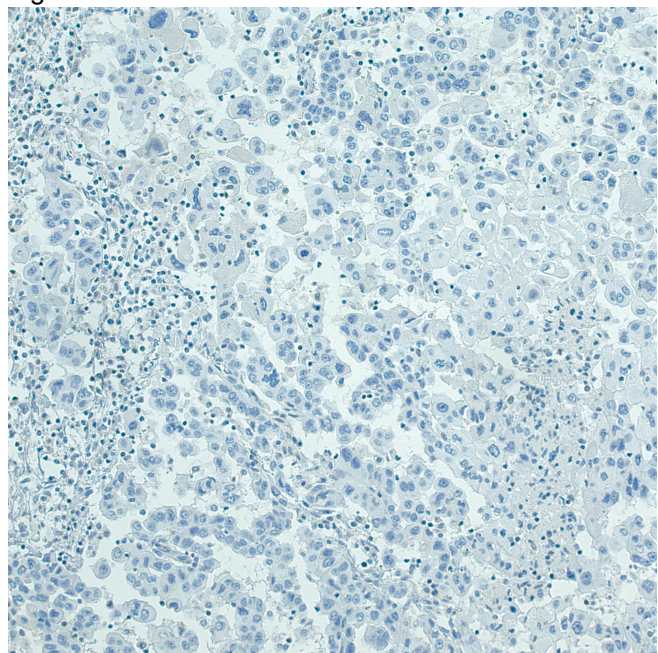
Figure 1 - 916

Figure 2 - 916

Conclusions: NF2 may be a useful sensitive immunohistochemical marker for distinguishing mesothelioma form reactive mesothelial proliferations. Further study of NF2 IHC expression as a diagnostic marker and its potential utility to guide targeted therapy might be of interest in the future.

917 HER2 (ERBB2) Immunohistochemistry in Non-Small Cell Lung Cancer: Does Expression Correlate with ERBB2 Mutational Status?

Anthony Cardillo[1], Sierra Kovar[1], David Hicks[1], Moises Velez[1]
[1]University of Rochester Medical Center, Rochester, NY

Disclosures: Anthony Cardillo: None; Sierra Kovar: None; David Hicks: None; Moises Velez: None

Background: *ERBB2* is an oncogene known for its sensitivity to tratuzumab and lapatinib in breast cancer. Non-small cell lung carcinomas (NSCLCs) uncommonly harbor *ERBB2* mutations, with trials underway to assess for targeted response. We sought to characterize three well known HER2 immunohistochemical (IHC) clones in the detection of *ERBB2* protein expression in NSCLC with *ERBB2* alterations, detected by next-generation sequencing (NGS). Expression was graded using the breast and gastric HER2 scoring systems to determine correlation with mutations. We assessed for cross-reactivity among additional molecular mutations, including *BRAF*, *KRAS*, *MET*, *NRAS*, and *EGFR*, along with reactivity to specimens without reportable mutations by NGS ("pan-negative").

Design: NSCLC specimens were retrieved with the following criteria: 1) Eight cases had a mutation/amplification of the ERBB2 gene detected by NGS and 2) Twenty-two pan-negative control specimens were stained, along with twenty-four specimens with a mutation in BRAF, KRAS, MET, NRAS, or EGFR allowing for determination of specificity and sensitivity. Three HER2 IHC clones were analyzed: Dako-AutoStainer Link 48: HercepTest™, Roche-Ventana: clone4B5, and Leica-Bond: cloneCB11. Each clone was graded by both the breast and gastric scoring systems as described by the College of American Pathologist (CAP). Correlations were assessed using Barnard's test, and confidence intervals (95%) were obtained using Wilson's method.

Results: The Dako clone showed any degree of staining in 3/8 of ERBB2-mutant specimens, a sensitivity of 38%. It showed staining in 7/45 non-ERBB2-mutant specimens. Thus, the specificity is 38/45, or 84% (95% CI, 71%-92%).
The Ventana clone (4B5) showed staining in 7/8 of ERBB2-mutant specimens, a sensitivity of 88% (95% CI, 53 – 98%). It showed staining in 32/43 non-ERBB2-mutant specimens. Thus, the specificity is 11/43, or 26% (95% CI, 15 – 40%).
The Leica clone (CB11) showed staining in 8/8 of ERBB2-mutant specimens, a sensitivity of 100% (95% CI, 68 – 100%). It showed staining in 36/45 non-ERBB2-mutant specimens. Thus, the specificity is 9/45, or 20% (95% CI, 11 – 34%).

Using the gastric and breast scoring systems, the accuracy of the Dako clone is 18/29, or 62% (95% CI, 44 – 77%) in both systems. The accuracy of clone 4B5 for the gastric system is 15/25, or 60% (95% CI, 41 – 77%), while the accuracy for the breast system is 16/25, or 64% (95% CI, 45 – 70%). The accuracy of clone CB11 for the gastric system is 18/29, or 62% (95% CI, 44 – 77%), while the accuracy for the breast system is 20/29, or 69% (95% CI, 51 – 84%).

Figure 1) The sensitivity and false positivity (1 – specificity) were plotted in ROC space. All three IHC clones fell below the line of no discrimination, which implies worse performance than random guessing.

Figure 1 - 917
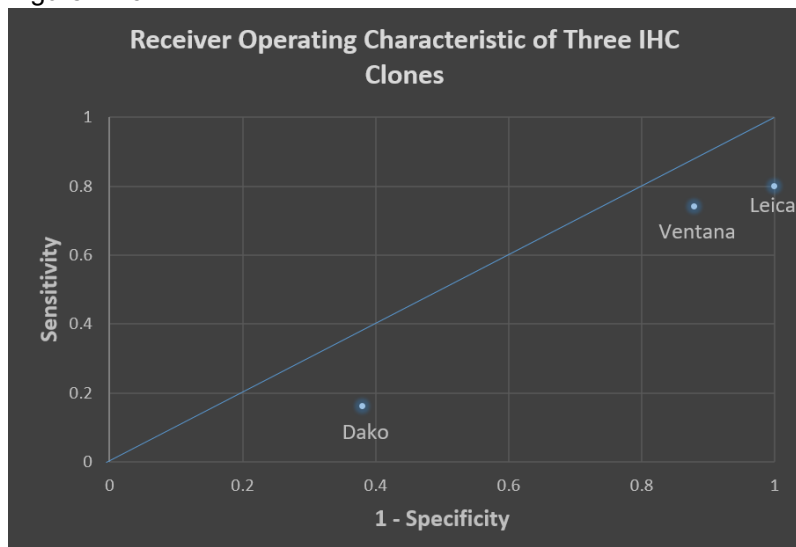
Conclusions: IHC is cheaper for screening mutations than NGS. An ERBB2 stain with the proper sensitivity and specificity would play a pivotal role in future workflows before reflexing to NGS. This study shows that at this time, no commercially available ERBB2 IHC clones are suitable for this purpose when using established grading systems, or using presence of staining alone.

918 Characterizing the Distribution of Molecular Mutations in Malignant Mesothelioma and Correlation to Morphology

Heather Chen[1], Melissa Tjota[2], Aliya Husain[1], Jefree Schulte[3]
[1]University of Chicago, Chicago, IL, [2]University of Chicago Medical Center, Chicago, IL, [3]University of Wisconsin-Madison, Madison, WI

Disclosures: Heather Chen: None; Melissa Tjota: None; Aliya Husain: None; Jefree Schulte: None

Background: Malignant mesothelioma (MM) is a lethal disease arising from the serosal membranes of the pleural and peritoneal cavities. Through genetic sequencing, a number of recurrent mutations have been identified in pleural and peritoneal MMs, most commonly *BAP1*, *NF2*, and *CDKN2A*. In this study, we aim to subcategorize MMs by their pathogenic mutations, and to determine if morphology features that correlate with genetic findings.

Design: MMs that had undergone next generation sequencing (NGS) at our institution between April 2013 and August 2020 were identified. All histologic diagnoses were originally made by thoracic pathologists from one institution. Ninety-six MMs arose from the pleura and 36 MMs arose from the peritoneum. Procedure performed and MM histiotype, were recorded. For epithelioid MMs, nuclear grade and architecture pattern were also recorded.

From our next generation sequencing panel, MMs were organized by categories of pathogenic mutations. A mutation was considered pathogenic if it had been included in the COSMIC database. We also included variants of unknown significance for mutations in *BAP1*, *CDKN2A*, and *NF2*.

Results: Results are summarized in table 1. There were 132 MMs identified (110 epithelioid MMs, 18 biphasic MMs, and 4 sarcomatoid MMs). The majority of the molecular material came from video-assisted thoracoscopic biopsies (31%) or surgical resections (38%). One-hundred-nine epithelioid MMs were graded, and the majority were low-grade (69%). One-hundred-four epithelioid MMs had architectural patterns recorded and the most commonly encountered pattern was solid (57%). The most common mutation for epithelioid MMs was *BAP1* (54%, n=59), of which 40 had mutations in additional genes. Of the biphasic MMs, 8 (44%) had at least a *BAP1* mutation with 6 of these cases having an additional pathogenic mutation. Of the sarcomatoid MMs (n=4), two (50%) had *NF2* and *CDKN2A* mutations. There were no differences in the distribution of mutations between histologic

subtypes (P=.14), and between high and low grade epithelioid MMs (P=.16). Solid growth pattern was more likely to have a mutation in TP53, while tubulopapillary pattern was more likely to not show any pathologic mutation/no mutations identified (P=.001). There were no differences in the proportion of cases with/without TP53 mutations in regard to morphologic subtype (P=.75) and nuclear grade (P=.23).

Key	Histiotype	Epithelioid Grade	Epithelioid Pattern						
	Epithelioid (n=110)	Biphasic (n=18)	Sarcomatoid (n=4)	HG (n=34)	LG (n=75)	Tubulopapillary (n=19)	Trabecular (n=17)	Adenomatoid (n=9)	Solid (n=59)
No pathogenic mutations/No Mutations Identified	19	3	0	6	13	5	3	1	9
BAP mutation(s) only	19	2	0	3	16	3	5	3	7
BAP mutation and mutation in 1 other gene	28	2	1	3	25	9	6	1	12
BAP mutation and mutation in 2 other genes	4	4	0	3	1	0	0	1	3
BAP mutation and mutation in 3 other genes	7	0	0	4	3	0	0	2	6
BAP mutation and mutation in 4 other genes	1	0	0	0	1	0	0	0	1
TP53 mutation and/or mutation in other genes	12	2	0	5	7	0	2	0	9
CDKN2A mutation and/or mutation in other genes	2	3	0	2	0	0	0	0	1
NF2 mutation and/or mutation in other genes	8	1	0	4	4	1	1	1	5
TP53 mutation and CDKN2A mutation	2	0	0	2	0	0	0	0	2
CDKN2A mutation and NF2 mutation	2	1	1	1	1	0	0	0	2
TP53 mutation and NF2 mutation	1	0	0	0	1	1	0	0	0
TP53 mutation, CDKN2A mutation, and NF2 mutation	1	0	1	0	1	0	0	0	1
Other Mutations (DDX3X, ATM, OR TERT)	4	0	1	1	2	0	0	0	1

Conclusions: The most common mutations across all histologic subtypes were *BAP1*, *CDKN2A, TP53*, and *NF2*, consistent with previous literature. Mutational status may correlate with architectural patterns, as TP53 mutation appears to be more often associated with solid growth pattern. This is the first attempt to correlate the prognostic histopathologic parameters with mutational status, and these findings suggest that a potential link exists between architectural patterns and mutational status; further study and characterization of the results is ongoing.

919   Validation of Urovysion as an Ancillary Tool for the Diagnosis of Mesothelioma in Surgical and Cytology Specimens

Julia Dahl[1], Michael Carter[2], Tao Huang[3], Kristine Konopka[1], Bryan Betz[3], Lindsay Kochan[4], Jeffrey Myers[1], Noah Brown[3]
[1]Michigan Medicine, Ann Arbor, MI, [2]NSHA, Halifax, Canada, [3]University of Michigan, Ann Arbor, MI, [4]Michigan Medicine, University of Michigan, Ann Arbor, MI

Disclosures: Julia Dahl: None; Michael Carter: None; Tao Huang: None; Kristine Konopka: None; Bryan Betz: None; Lindsay Kochan: None; Jeffrey Myers: None; Noah Brown: None

Background: Mesothelioma is an uncommon but aggressive malignancy for which mortality is projected to peak in the next decade. Diagnosis can be challenging, especially in cytology and small biopsy specimens. UroVysion is a multi-probe FISH assay that focuses on aneuploidy in chromosomes 3, 7 and 17, and 9p21 deletion as features of malignancy. We examine the diagnostic utility of UroVysion in cytological and tissue diagnosis of mesothelioma.

Design: Formalin-fixed, paraffin-embedded (FFPE) surgical pathology and pleural effusion cytology specimens reporting benign and malignant mesothelial proliferations were identified within a single institution laboratory information system. Materials were retrieved from tissue archives and routinely stained tissue and cell block slides were reviewed for diagnosis. Areas of mesothelial proliferation were identified and marked. The UroVysion assay was performed with modifications for FFPE tissue. Within the areas marked by reviewing pathologists, fifty (50) consecutive mesothelial cells were independently scored by two technologists. Cutoff values were generated from positive and negative controls. Cases were scored as positive if ≥ 10/100 cells had no (zero) 9p21 signals, or ≥ 10/100 cells had gains for ≥ 2 chromosomal probes.

Results: The study set comprised 36 pleural effusion cell blocks (negative-11, atypical-6, suspicious-1, positive-2) and 29 surgical specimens (benign hyperplasia-12, mesothelioma-17). UroVysion was positive in 10 of 16 (63%) evaluable cytology specimens from patients with tissue diagnoses of mesothelioma (aneuploid+9p21 deletion-4, aneuploid only-3, 9p21 deletion only-3) including specimens originally interpreted as negative (3), atypical (4), suspicious (1), and positive (2). Four cytology specimens from patients with biopsy proven mesothelioma were insufficient for analysis. UroVysion was positive in 12 (71%) of 17 surgical specimens with mesothelioma (aneuploidy+9p21 deletion-6, aneuploidy only-1, 9p21 only-5). No false positives occurred in either group (100% specificity). The use of UroVysion rather than 9p21 alone resulted in increased sensitivity (63% versus 44% for cytology specimens, 71% versus 65% for surgical specimens).

Conclusions: UroVysion is a specific and relatively sensitive diagnostic tool for separating benign from malignant mesothelial proliferations in cytology and surgical FFPE specimens. This approach is more sensitive than 9p21 FISH alone.

920   Expression of Delta-Like Ligand 3 in Thoracic Neuroendocrine Neoplasms: New insights into a Novel Diagnostic and Therapeutic Target

Alexandra Danakas[1], Moises Velez[1], Chauncey Syposs[1], Donna Russell[1], Sachica Cheris[1], Tanupriya Agrawal[1]
[1]University of Rochester Medical Center, Rochester, NY

Disclosures: Alexandra Danakas: None; Moises Velez: None; Chauncey Syposs: None; Donna Russell: None; Sachica Cheris: None; Tanupriya Agrawal: None

Background: Small cell lung cancer (SCLC) represents approximately 15% of all primary lung cancers. Despite the aggressive nature of advanced SCLC, limited second-line therapeutic options beyond checkpoint inhibitors exist.

Delta-like ligand 3 (DLL3) is an inhibitory Notch ligand which promotes neuroendocrine (NE) tumorigenesis, with recent studies showing that DLL3 is highly expressed in SCLC. The DLL3 expression profile has facilitated the development of new treatment options that use DLL3 to specifically target SCLC cells. There are few studies investigating the role of DLL3 in SCLC, while the literature on other NE tumors is very limited. We aim to provide

new insights to the role of DLL3 in identifying NE differentiation and its usefulness as a targeted therapy for NE tumors.

Design: We identified 72 cases of primary lung tumors diagnosed at our institution from 2016-2020 including both biopsy and resection specimens. These included 33 carcinoid tumors (26 typical and 7 atypical), 12 large cell neuroendocrine carcinomas (LCNEC), 18 SCLC, 2 combined small cell carcinoma and LCNEC, 3 adenocarcinomas and 4 squamous cell carcinomas (SCC). Tissue sections were stained with VENTANA DLL3 (SP347) assay using the recommended staining conditions and tissue controls. DLL3 expression in tumor cells were classified as high expression (≥50%), low (1-49%), or negative (<1%) for expression (Figure 1).

Results: Positive staining, including high or low expression of DLL3, was found in 58 of the primary lung neoplasms tested, all with NE differentiation. DLL3 expression was present in 73% of typical carcinoid tumors, 71% of atypical carcinoid tumors, all LCNEC and SCLC. No expression was identified in the adenocarcinoma or SCC cases (Table 1). The sensitivity of DLL3 expression is 88%, with a specificity of 100%.

Table 1: DLL3 expression in lung primary neoplasms

Tumor Type	DLL3 Negative n (%)	DLL3 Low Expression n (%)	DLL3 High Expression n (%)
Typical Carcinoid (n=26)	7 (27)	6 (23)	13 (50)
Atypical Carcinoid (n=7)	2 (29)	1 (14)	4 (57)
Large Cell Carcinoma (n=12)	0 (0)	0 (0)	12 (100)
Small Cell Carcinoma (n=18)	0 (0)	4 (22)	14 (78)
Combined Large and Small cell carcinoma (n=2)	0 (0)	0 (0)	2 (100)
Adenocarcinoma (n=3)	3 (100)	0 (0)	0 (0)
Squamous Cell Carcinoma (n=4)	4 (100)	0 (0)	0 (0)

Figure 1 - 920
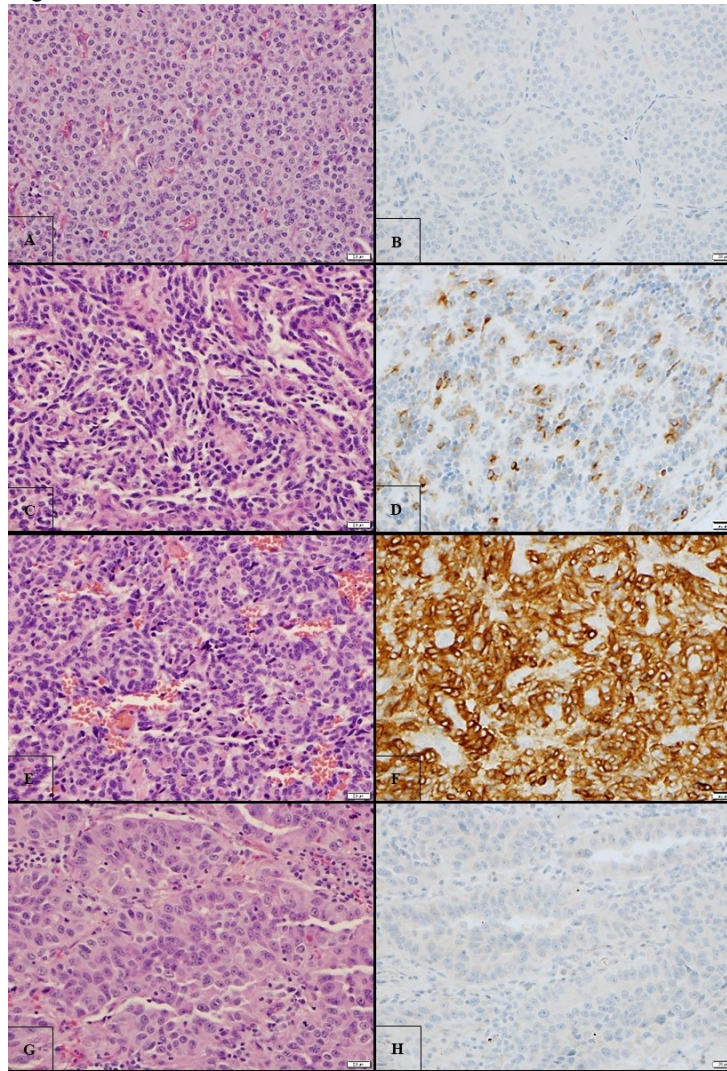
Figure 1 legend: Typical carcinoid tumor (H&E, A) with no DLL3 expression (B); Typical carcinoid tumor (H&E, C) with low DLL3 expression (D); Typical carcinoid tumor (H&E, E) with high DLL3 expression (F); Adenocarcinoma (H&E, G) with no DLL3 expression (H). All photomicrographs taken at 400X.

Conclusions: Our study shows DLL3 expression is comparable to other frequently used NE markers. It shows high expression in SCLC and LCNEC, with a variable expression in majority of carcinoid tumors.   DLL3 can be potentially used as a diagnostic marker and a potential therapeutic target for patients with neuroendocrine neoplasms, especially in those with DLL3 high expression, which is observed in all SCLC and LCNEC patients.

921 Comparison of Diagnostic Utility of Delta-Like Ligand 3 to Insulinoma-Associated protein 1 (INSM1) in Neuroendocrine Neoplasms of Lung

Alexandra Danakas[1], Moises Velez[1], Chauncey Syposs[1], Sachica Cheris[1], Tanupriya Agrawal[1]
[1]University of Rochester Medical Center, Rochester, NY

Disclosures: Alexandra Danakas: None; Moises Velez: None; Chauncey Syposs: None; Sachica Cheris: None; Tanupriya Agrawal: None

Background: Delta-like ligand 3 (DLL3) is a Notch pathway ligand that has been found to be expressed on the cell surface of small cell lung carcinoma (SCLC) as well as other neuroendocrine (NE) tumor cells. DLL3 acts as an inhibitory ligand of NOTCH receptors which regulate neuroendocrine differentiation. Insulinoma-associated protein 1 (INSM1) is a zinc-finger transcription factor that is involved in the development of NE differentiation in tissues. This study aims to compare expression of DLL3 antibody to INSM1 in neuroendocrine neoplasms of lung origin.

Design: We identified 70 cases of primary lung tumors from 2016-2020 including biopsy and resection specimens. These included 33 carcinoid tumors (26 typical and 7 atypical), 12 large cell neuroendocrine carcinomas (LCNEC), 16 SCLC, 2 combined small cell carcinoma and LCNEC, 3 adenocarcinomas and 4 squamous cell carcinomas (SCC). The tumors met the classification requirements detailed in the 2015 WHO Classification for thoracic tumors. Tissue sections were stained with VENTANA DLL3 clone SP347 Assay and INSM1 antibody clone A-8 from Santa Cruz Biotechnology, optimized for use on the Ventana platform. Ventana DLL3 (SP347) was optimized using the recommended staining conditions and tissue controls. Immunohistochemical expression of DLL3 and INSM1 was classified as either positive or negative.

Results: DLL3 expression was present in all SCLCs and LCNECs, including the combined neoplasms, which correlated to INSM1 expression, with the exception of one LCNEC in which INSM1 was negative. All lung neoplasms tested without NE differentiation were negative for both DLL3 and INSM1. Variations in DLL3 expression were identified among the carcinoid tumors, whereas INSM1 was positive in all typical carcinoid tumors (100%) with the exception of one atypical carcinoid tumor or 86% showing expression (Figures 1 & 2). The sensitivity of INSM1 (97%) was higher than DLL3 (83%), both markers were found to have 100% specificity for NE differentiation (Table 1).

Table 1: DLL3 and INSM1 Expression in Primary Lung Neoplasms

Tumor type	DLL3 Positive n (%)	DLL3 Negative n (%)	INSM1 Positive n (%)	INSM1 Negative n (%)
Typical Carcinoid (n=26)	19 (73)	7 (27)	26 (100)	0 (0)
Atypical Carcinoid (n=7)	3 (43)	4 (57)	6 (86)	1 (14)
Large Cell Carcinoma (n=12)	12 (100)	0 (0)	11 (92)	1 (8)
Small Cell Carcinoma (n=16)	16 (100)	0 (0)	16 (100)	0 (0)
Combined Large and Small Cell Carcinoma (n=2)	2 (100)	0 (0)	2 (100)	0 (0)
Adenocarcinoma (n=3)	0 (0)	3 (100)	0 (0)	3 (100)
Squamous Cell Carcinoma (n=4)	0 (0)	4 (100)	0 (0)	4 (100)
Sensitivity	83%		97%	
Specificity	100%		100%	

Figure 1 - 921
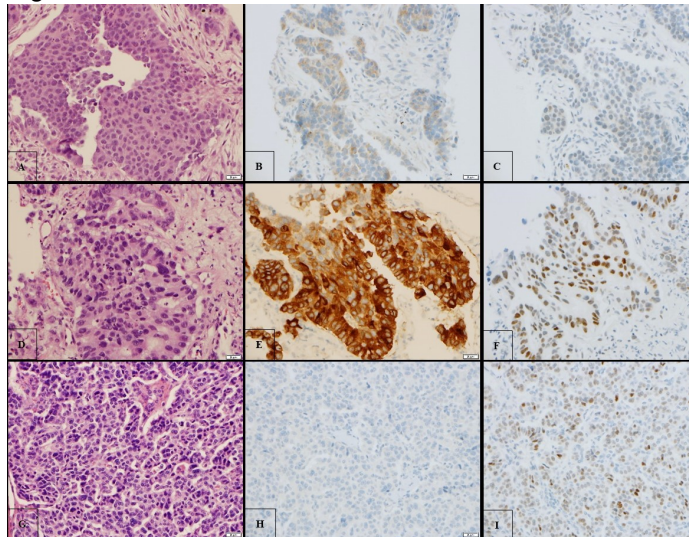
Figure 1 Legend: Atypical carcinoid tumor (H&E, A) with DLL3 expression (B) and no INSM1 expression (C); Large cell carcinoma (H&E, D) with DLL 3 (E) and INSM1 (F) expression; Typical carcinoid tumor (H&E, G) with no DLL3 expression (H) and present INSM1 expression (I). All photomicrographs taken at 400x.

Figure 2 - 921

Tumor Type	DLL3 and INSM1 Positive n (%)	DLL3 Positive/INSM1 Negative n (%)	DLL3 Negative/INSM1 Positive n (%)	DLL3 and INSM1 Negative n (%)
Typical Carcinoid (n=26)	19 (73)	0 (0)	7 (27)	0 (0)
Atypical Carcinoid (n=7)	3 (43)	0 (0)	3 (43)	1 (14)
Large Cell Carcinoma (n=12)	11 (92)	1 (8)	0 (0)	0 (0)
Small Cell Carcinoma (n=16)	16 (100)	0 (0)	0 (0)	0 (0)
Combined Large and Small Cell Carcinoma (n=2)	2 (100)	0 (0)	0 (0)	0 (0)
Adenocarcinoma (n=3)	0 (0)	0 (0)	0 (0)	3 (100)
Squamous Cell Carcinoma (n=4)	0 (0)	0 (0)	0 (0)	4 (100)

Figure 2 Legend: Discordant cases highlighted: No DLL3 expression (green); No expression of both DLL3 and INSM1 (blue); No INSM1 expression only (yellow).

Conclusions: The sensitivity of DLL3 is slightly lower in our cohort in comparison to that of INSM1, due to the variable expression among carcinoid tumors, though notably there have been some studies which also identified a similar finding in INSM1 expression for carcinoid tumors. Our findings show the sensitivity of DLL3 is comparable to other frequently used markers of NE differentiation, synaptophysin, chromogranin and CD56. Furthermore, DLL3 shows promise in being a reliable diagnostic marker and therapeutic target for lung neuroendocrine neoplasm, predominantly in SCLC and LCC where expression was found in 100% of cases.

922   Pembrolizumab Plus Radiation and Chemotherapy for Stage IV Lung Adenocarcinoma in the Regional VA Healthcare System, Western New York (VAWNY)

Liang Ding[1], Yujie Zhang[1], Ayesha Arshad[2]
[1]University at Buffalo, NY, [2]VAWNY, Buffalo, NY

Disclosures: Liang Ding: None; Yujie Zhang: None; Ayesha Arshad: None

Background: In the KEYNOTE-189 trial, pembrolizumab plus chemotherapy significantly improved overall survival (OS) in patients having metastatic non-small-cell lung carcinoma (NSCLC) regardless of tumor Programmed Death Ligand-1 (PD-L1) expression. Other studies have shown that radiotherapy upregulates PD-L1 expression, resulting in a better prognosis for those patients receiving radiotherapy before PD-L1 blockade; however, potential toxicity increases when pembrolizumab is combined with radiation and chemotherapy. Whether this combination improves survival for patients with advanced NSCLC is unclear.

Design: Data were collected and studied retrospectively for NSCLC patients at VAWNY tested for PD-L1 expression from 2016 to 2019 (Table 1, n=283). A subset of patients having EGFR and ALK un-mutated, stage IV, lung adenocarcinoma was defined for survival analysis (n=119). These patients were treated with radiation and concurrent platinum-doublet chemotherapy with or without pembrolizumab. They were stratified into three groups based on the PD-L1 tumor proportion score (TPS). OS was defined as the interval between first treatment cycle and death for up to 24 months follow-up. Kaplan-Meier methods, the log-rank test, and Cox proportional hazard models were used for statistical analysis.

Results: As shown in Figure 1, estimated median OS (95% CI) was > 24 months in the pembrolizumab group versus 11(8.0 to 14.0) months in the control group (hazard ratio [HR], 0.35; 95% CI, 0.22 to 0.60, p = 0.000009). About 36.6% of patients had PD-L1 TPS <1%; 34.5% had PD-L1 TPS of 1% - 49%; and 28.9% had PD-L1 TPS >50%. In the group of negative PD-L1 expressing tumors (<1%), no statistically significant survival difference was found between the pembrolizumab subgroup and the control subgroup. In the group of median-low PD-L1 expressing tumors (1% - 49%), estimated median OS (95% CI) was 22 (13.3 to 30.7) months in the pembrolizumab subgroup versus 11 (6.7 to 15.3) months in the control subgroup (HR, 0.44; 95% CI, 0.19 to 0.92, p = 0.04). In the group of high PD-L1 expressing tumors (>50%), the estimated median OS (95% CI) was greater than 24 months in the pembrolizumab subgroup versus 10 (3.5 to 16.5) months in the control subgroup (HR, 0.22; 95% CI, 0.10 to 0.63, p = 0.002). In pembrolizumab-treated patients, OS differences between the PD-L1 high-expressing (>50%) and low-expressing (1-49%) groups were not statistically significant (p=0.13), but these differences were significant between the high-expressing and non-expressing groups (p = 0.03).

Table 1. Non-small-cell lung carcinoma patients at VAWNY tested for PD-L1 expression.	
Patient (n= 283)	N (%) (year 2016 - 2019)
Age (median age 71) 50 – 70 71 – 90	 134 (47.3%) 149 (52.7%)
Gender Male Female	 275 (97%) 8 (3%)
Histology Adenocarcinoma Squamous cell carcinoma Other	 206 (72.7%) 58 (20.5%) 19 (6.8%)
Smoker (former and current) Non-smoker	232 (82%) 51 (18%)
EGFR/ALK mutations With Without	 8 (2.8%) 275 (96.7%)
Stage I II III IV	 41 (15%) 24 (9%) 33 (12%) 185 (63.1%)

PD-L1 TPS (tumor proportion score)	
< 1%	104 (36.6%)
1-49%	98 (34.5%)
>50%	81 (28.9%)
Treatment (stage IV, adenocarcinoma)	N=119 (year 2016 - 2018)
Rad + Chem + Pem (Pem group)*	56
Rad + Chem (Control group)	63
* Rad: radiation;Chem: chemotherapy; Pem:Pembrolizumab.	

Figure 1 - 922
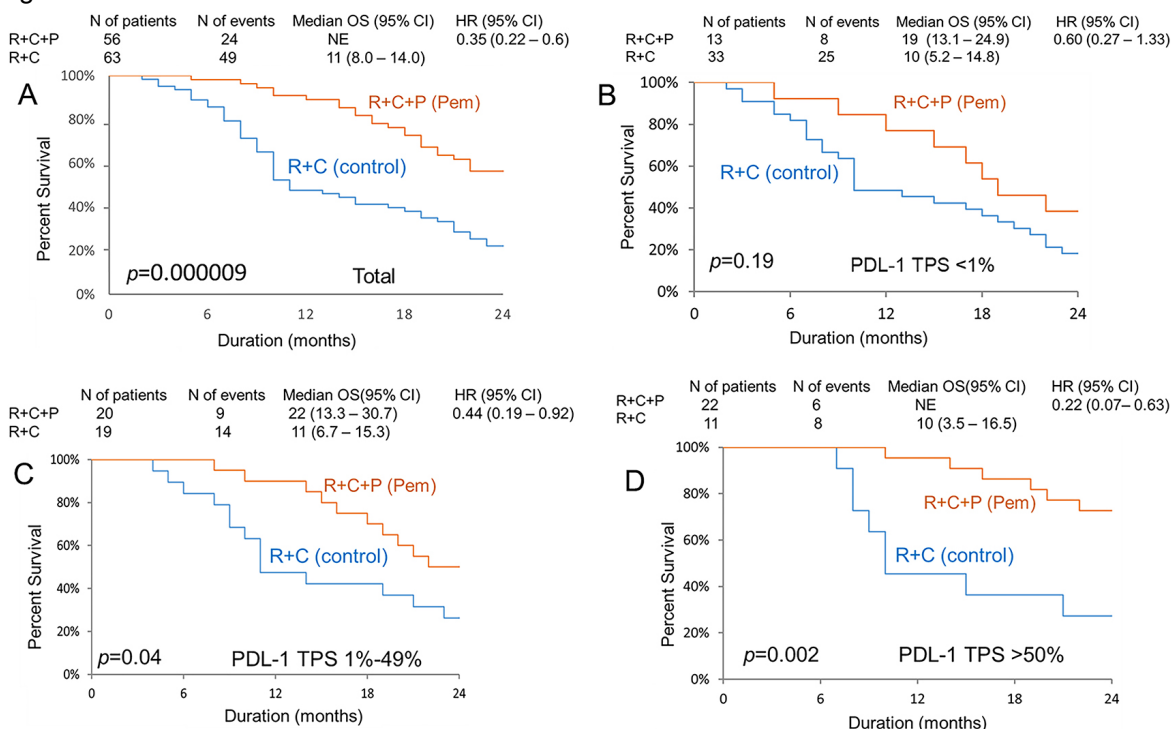
Figure 1. Kaplan-Meier analysis of overall survival (OS) in the (A) total group and in subsets of patients by tumor proportion score (TPS): (B) <1%, (C) 1%-49%, and (D) >50%. HR, hazard ratio; NE, value could not be estimated. R: radiation;C: chemotherapy; P or Pem:Pembrolizumab.

Conclusions: Pembrolizumab plus radiation therapy and concurrent platinum-doublet chemotherapy demonstrates significantly improved OS in EGFR and ALK wild-type, stage IV, lung adenocarcinoma. Patients whose tumors displayed high levels of PD-L1 expression benefitted more from pembrolizumab than those whose tumors were negative.

923   Biomarker Testing in Non-Small Cell Lung Carcinoma: Performance and Patient Outcomes

Saleh Fadel[1], Venus Chirip[2], Paul Wheatley-Price[3], Neil Reaume[3], Bryan Lo[1], Nina Chang[4], Harmanjatinder Sekhon[4], Marcio Gomes[1]
[1]The Ottawa Hospital, University of Ottawa, Ottawa, Canada, [2]The Ottawa Hospital, Eastern Ontario Regional Laboratory Association, Ottawa, Canada, [3]The Ottawa Hospital, Ottawa, Canada, [4]The Ottawa Hospital, University of Ottawa, Eastern Ontario Regional Laboratory Association, Ottawa, Canada

Background: Approximately 70% of non-small cell lung carcinomas (NSCLC) are diagnosed at stage III/IV, leading to poor five-year survival rates of 19%. The survival is particularly poor without treatment. Predictive biomarker

testing for metastatic NSCLC is now the standard of practice and an essential component of treatment planning. Lacking knowledge of predictive biomarker test results at initial oncology consultation can therefore be a major factor precluding a timely management decision. At our institution, we implemented a hybrid reflex testing system for NSCLC predictive biomarkers and yet we encountered cases where test results were unavailable at the initial medical oncology consultation.

Design: We conducted a diagnostic assessment of 100 consecutive NSCLC samples evaluating the fidelity of predictive biomarker testing guideline implementation, three quality dimensions (effectiveness, efficiency and timeliness), and patient care outcomes.

Results: 100 lung cancer samples corresponded to 93 patients. **Implementation**: Testing guideline was not followed in 25 cases, with 8 cases (32%) having no or incomplete set of biomarkers ordered and 7 cases (28%) having biomarkers ordered on non-cytology samples of early stage disease. **Effectiveness**: For treatment planning, stage IV squamous cell NSCLC requires PDL1 testing, and stage IV non-squamous NSCLC requires EGFR, ALK, ROS1, and PDL1 testing. Of 24 stage IV cases referred to medical oncology, 13 (54.2%) had all relevant biomarker results available at first consultation. Of 69 non-metastatic cases (where biomarker testing was not clinically relevant), 45 cases (65.2%) had at least one test performed. **Efficiency**: Inefficient testing occurred in 3 cases of misuse (1 duplicate and 2 on ineligible tumor types). **Timeliness**: Reflex biomarker testing occurred in 50/56 appropriate cases (91.3%). The turn-around time for biomarker test reporting was (mean ± standard deviation in days): EGFR=11.1 (±4.4), PD-L1=6.2 (± 4.1), ALK=2.9 (±2.2), ROS=7.1 (±6.4). **Patient care outcomes**: Out of 66 patients who were referred to medical oncology, 36 (54.5%) had a treatment decision made on the first visit. In the remaining 30 cases, the main reason for a delayed treatment decision was unclear stage in 12 cases (40%). Lack of biomarker results was the sole reason for a delayed treatment decision in 4 cases (13.3%) and was a contributing factor in 3 others (10%).

Conclusions: Multiple factors, including biomarker testing, impact the ability to make a timely management plan. Our study showed that some biomarker testing issues related to fidelity of implementation, quality, and patient care outcomes persist even after adoption of reflex testing guidelines. As NSCLC biomarkers and treatment algorithms become more complex, the design of rapidly adaptive systems is required.

924 Predictors of Upgrading Diffuse Malignant Mesothelioma from Epithelioid to Biphasic from Initial Sampling to Extended Pleural Decortication

Rachel Fanaroff[1], Janina Markidan[2], Naomi Hardy[2], Grace Patrice Anyetei-Anum[2], Melissa Culligan[1], Erica Glass[2], Teklu Legesse[3], Joseph Friedberg[1], Allen Burke[4]
[1]University of Maryland, Baltimore, MD, [2]University of Maryland Medical Center, Baltimore, MD, [3]UMMC, [4]University of Maryland Medical School of Medicine, Baltimore, MD

Disclosures: Rachel Fanaroff: None; Janina Markidan: None; Naomi Hardy: None; Grace Patrice Anyetei-Anum: None; Erica Glass: None; Teklu Legesse: None; Joseph Friedberg: None; Allen Burke: None

Background: The presence of a sarcomatoid component to a malignant mesothelioma in a pleural biopsy is often a contraindication to surgery. In some cases, initial sampling shows only an epithelioid component, but a sarcomatoid element is seen at resection, upgrading the tumor from purely epithelioid to biphasic. The purpose of this study was to determine the features associated with upgraded subtyping, with an emphasis on the presence of a transitional growth pattern, a recently described entity.

Design: Features of tumors that were upgraded were compared to those that were not using the following parameters: type of biopsy, number of blocks processed, degree of solid growth (scored from 0-4), and degree of transitional growth (scored from 0-2). As a secondary outcome, survival of both groups was evaluated by Kaplan-Meier analysis.

Results: Thirty-eight biopsy and extended pleural decortication pairs from 2015 to the present were retrospectively evaluated. Initial sampling included 9 transcutaneous biopsies, 25 open biopsies, and 4 partial pleurectomies. All initial samples were subtyped as epithelioid. The group that was upgraded was designated group A (n=8), while the group that was not upgraded was designated group B (n=30). The presence of any transitional growth pattern was associated with upgrading (p=0.0008). Additionally, the degree of transitional growth was greater in group A than in

group B (group A mean score 1.8, group B mean score 0.4, p=0.0002). There was a trend of increased solid growth in group A (p=0.09). There was no significant difference between initial sampling type between groups A and B, although none of the partial pleurectomies were upgraded. The number of blocks processed was not significant. Group B demonstrated worse survival (p<0.001, Figure 1).

Figure 1 - 924
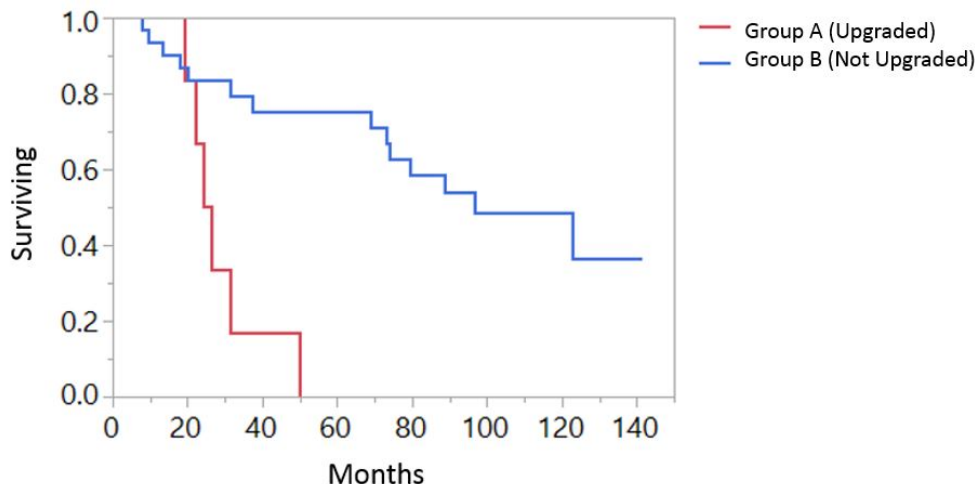
Conclusions: In this study, the presence of a transitional growth pattern increased the risk of upgrading from the epithelioid to biphasic subtype, and survival was worse in this group. Reporting of any transitional component in a biopsy should be considered.

925   Interpretation of Methylthioadenosine Phosphorylase (MTAP) Expression by Immunohistochemistry in Malignant Pleural Mesothelioma is Improved with Monoclonal Antibody 1813 Compared to Monoclonal Antibody EPR6893

Christopher Febres-Aldana[1], Achim Jungbluth[1], Prasad Adusumilli[1], Darren Buonocore[1], Jason Chang[1], Denise Frosina[1], Jerica Geronimo[1], Enmily Hernandez[1], Michael Offin[1], Natasha Rekhtman[1], William Travis[1], Marjorie Zauderer[1], Soo-Ryum Yang[1], Marc Ladanyi[1], Jennifer Sauter[1]
[1]Memorial Sloan Kettering Cancer Center, New York, NY

Background: Co-deletions of *MTAP* occur in most tumors with *CDKN2A*/p16[INK4a] deletions, alterations that are enriched in malignant pleural mesothelioma (MPM) and not detected in benign mesothelial proliferations. MTAP immunohistochemistry (IHC), often with monoclonal antibody (mAb) EPR6893 (ab126770, Abcam), is increasingly used in diagnostic pathology as a surrogate marker for CDKN2A deletions to support a diagnosis of MPM. In our experience, interpretation of this mAb can be challenging. Testing different mAbs and comparison with targeted next-generation sequencing (NGS) data may improve interpretation and understanding of MTAP expression by IHC.

Design: MTAP IHC (mAbs EPR6893 and 1813 (NBP2-75730, Novus); 83 and 49 cases, respectively) was performed retrospectively on FFPE tissue from 83 MPM (68 epithelioid, 13 biphasic, and 2 sarcomatoid). Cytoplasmic MTAP expression was scored as retained, lost or equivocal. Stromal cells served as positive internal controls. NGS was performed on all 83 cases (all had adequate tumor purity (>20%)), and data were reviewed for

copy number abnormalities (CNA). Fold change > -1.6 in *CDKN2A/2B* loci was cutoff used to detect 9p21.3 deletion.

Results: There is a substantial proportion of equivocal cases with MTAP IHC: 16 (19%, n=83) and 5 (10%, n=49), mAbs EPR6893 and 1813, respectively. MAb 1813 showed stronger immunoreactivity, reducing non-specific staining often seen with mAb EPR6893 and facilitating better distinction of loss or retained expression (Figure 1 and 2). Nine equivocal cases with mAb EPR6893 showed loss of expression with mAb 1813, reducing equivocal cases from 14 (28%) to 5 (10%) in the subset (n=49) tested with both mAbs (Table 1). 9p21.3 deletions were detected by NGS in 4 of these 9 cases. All MPM with retained MTAP expression by IHC showed no CNA of 9p21.3A by NGS. However, a subset with loss of MTAP expression (26-36%) did not harbor 9p21.3 deletion by NGS.

Total cases	Anti-MTAP clone	MTAP expression by IHC (n, %)		9p21.3 deletion on MSK-IMPACT (n, %)	Fold Change (range (n))
83	EPR6893	Retained	40 (48%)	Deleted: 0	-
				Not deleted: 40 (100%)	1.5 (1)
		Loss	27 (33%)	Deleted: 18 (67%)	1.7 – 5.6
				Not deleted: 9 (33%)	1.6 (1)
		Equivocal	16 (19%)	Deleted: 6 (37%)	1.8 – 3.3
				Not deleted: 10 (63%)	-
49	EPR6893	Retained	16 (33%)	Deleted: 0	-
				Not deleted: 16 (100%)	1.5 (1)
		Loss	19 (39%)	Deleted: 14 (74%)	1.7—4.1
				Not deleted: 5 (26%)	-
		Equivocal	14 (28%)	Deleted: 5 (36%)	1.7– 3.3
				Not deleted: 9 (64%)	-
	1813	Retained	16 (33%)	Deleted: 0	-
				Not deleted: 16 (100%)	1.5 (1)
		Loss	28 (57%)	Deleted: 18 (64%)	1.7– 4.1
				Not deleted: 10 (36%)	-
		Equivocal	5 (10%)	Deleted: 1 (20%)	1.7 (1)
				Not deleted: 4 (80%)	

Figure 1 - 925

Figure 2 - 925

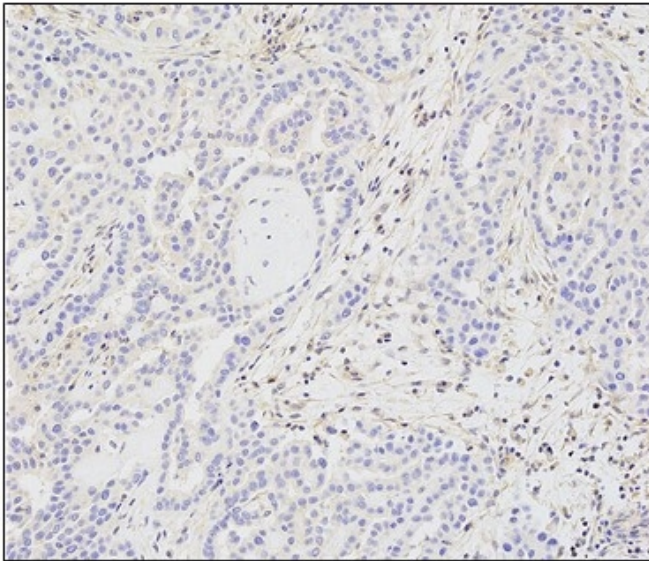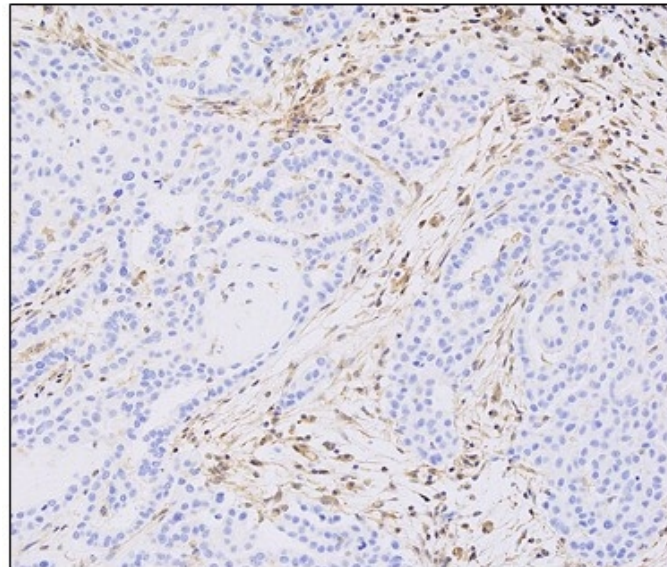Figure 1. Example of EPR6893 clone immunoreactivity in a MPM case with loss of MTAP expression, compared to figure 2

Figure 2. Example of 1813 clone immunoreactivity in a MPM case with loss of MTAP expression, compared to figure 1

Conclusions: In our experience, the MTAP mAb 1813 is easier to interpret, reducing equivocal interpretations, compared to mAb EPR6893. NGS detected a subgroup of MPM characterized by loss of MTAP expression with preserved 9p21.3 region. While *MTAP* deletions do occur in the absence of *CDKN2A/2B* deletions, repression of gene expression mediated by epigenetic mechanisms or post-translational events may be alternative explanations. Further molecular testing to detect alterations in *MTAP* and to explore these possibilities warrants further study.

926 Heterogeneity of Immune Biomarkers in Patients with Synchronous Lung Adenocarcinomas

Andréanne Gagné[1], Michèle Orain[2], Venkata Manem[2], Philippe Joubert[3]
[1]Laval University, Quebec City, Canada, [2]Institut Universitaire de Cardiologie et de Pneumologie de Quebec Research Center, Québec, Canada, [3]Quebec Heart and Lung Institute, Quebec, Canada

Disclosures: Andréanne Gagné: None; Michèle Orain: None; Venkata Manem: None; Philippe Joubert: None

Background: Patients with multiple synchronous lung adenocarcinomas (MSLA) are considered to harbor multiple independent primary cancers. This hypothesis is supported by the heterogeneity of genetic alterations between the tumors within the same patient reported in the literature. Even though the optimal treatment of MSLAs is surgical, immunotherapy could be used in patients for which it is contraindicated. Immune biomarkers, such as PD-L1 expression, tumor mutation burden (TMB) and T-cell repertoire (TCR), have not been explored in MSLAs and could be heterogeneous. We aimed to evaluate the heterogeneity of immune biomarkers between MSLAs.

Design: 34 patients that underwent a surgical resection for MSLAs between 2013 and 2016 in our center were selected. For each patient, three formalin-fixed paraffin embedded blocks were selected: one from two synchronous tumors and one from normal lung tissue. PD-L1 expression (22C3 pharmDx) was assessed with the tumor proportion score (TPS) at clinically relevant cut-offs (<1%, 1-49% and >50%). DNA was extracted and samples were subjected to whole-exome sequencing (Illumina HiSeq platform, Agilent SureSelect XT). Somatic variants (single nucleotide variants and insertion-deletions) were called using Strelka and MuTect. TMB was calculated for each MSLA. TCR predictions were done using the MiXCR pipeline. Descriptive statistics and Cohen's kappa were used to compare PD-L1 expression and TMB between MSLA pairs. Morisota's index was used as a measure of the similarity of the T-cell repertoire (0 indicates distinct TCR, while 1 indicates identical TCR).

Results: PD-L1 expression between the MSLAs was discordant in 21 (38%) patients (considering all cut-offs). A discrepancy was also observed for 16 patients (47.1%, k= -0.13) at TPS 1% cut-off and for 9 patients (26.5% k= 0.14) at TPS 50% cut-off. The median difference in TMB between the MSLAs of the same patient was 56% (range 2-95%). TCR was heterogeneous between MSLA pairs, as indicated by a median Morisota's index of 0.15 (range 0-0.65).

Conclusions: Similarly to genetic alterations, immune biomarkers were highly heterogeneous between MSLAs from the same patient, which suggests that immunotherapy could not be efficient in this population. Further studies are needed to explore other immune markers to better characterize the immune heterogeneity between MSLAs and its potential clinical impact.

927   Transcriptomic Signatures in EGFR Sensitive Non-Small Cell Lung Cancer Are Associated with Early vs Late Resistance to Tyrosine Kinase Inhibitors

Matthew Gayhart[1], Manuel Arana Rosainz[1], Arkadiusz Gertych[2], Chintda Santiskulvong[1], Eric Vail[1], Celeste Eno[1], Jianbo Song[1], Fabiola Medeiros[1], Jean Lopategui[3]
[1]Cedars-Sinai Medical Center, Los Angeles, CA, [2]3DHISTECH Ltd., Budapest, Hungary, [3]Cedars-Sinai Medical Center, West Hollywood, CA

Disclosures: Matthew Gayhart: None; Manuel Arana Rosainz: None; Arkadiusz Gertych: None; Chintda Santiskulvong: None; Eric Vail: None; Celeste Eno: None; Jianbo Song: None; Fabiola Medeiros: None; Jean Lopategui: None

Background: *EGFR* tyrosine kinase inhibitors (TKIs) have become an efficacious first line treatment option for *EGFR*-mutated non-small cell lung cancer (NSCLC) patients. However, resistance inevitably develops in patients treated with TKIs with a very wide range of time to relapse from a few months to several years (median 12 months). There is a clear clinical need for a method to assess which patients will respond long term to TKIs and which will relapse early and might benefit from other therapy. While the T790M and C797S mutations and *MET* and *HER2* amplifications have been identified as mechanisms of resistance, most factors for the wide variability of time to relapse are largely unknown. Using RNA expression analysis, we aim to explore the transcriptome of NSCLC to identify pathway regulators that are activated or inhibited in early versus late relapse patients.

Design: A total of 24 patients with *EGFR*-sensitive NSCLC and 9 normal lung samples were selected retrospectively. Formalin-fixed paraffin-embedded samples from the initial diagnosis were analyzed by RNA-Seq using Next-Generation Sequencing. The unsupervised principle component analysis (PCA) demonstrated separation of early (less than 12 months, n=13), late (12 or more months, n=11), and normal lung control samples (n=9). Differential expression (DE) analysis for pairwise comparisons between early relapse, late relapse, and normal lung was performed. Significant differentially expressed genes (Adjusted p< 5%) were selected as input for pathway analysis.

Results: On PCA, a distinct separation existed between normal lung, early relapsed NSCLC, and late relapsed NSCLC. In the comparison between early and late, there were a total of 63 DE genes, with 40 genes upregulated and 23 genes downregulated. An analysis of upstream regulators predicted significant activation of *TGFB-1, ERB2, PIK3CA,* and *BRD4* (activation z-score >2) in the early group and a significant inhibition of *TGFB-1, HRAS, SMAD7,* and *SPDF* (activation z-score <2) in the late group. Finally, a case by case transcriptome analysis identified 3 gene transcripts with a predominant significant upregulation in early (*MDK* and *CDC20*) and late relapse (*GRHL1*). The overall downstream functional effects were activation of cell movement and angioinvasion and inhibition of cell death pathways in early relapse NSCLC patients.

Figure 1 - 927

Principle Component Analysis
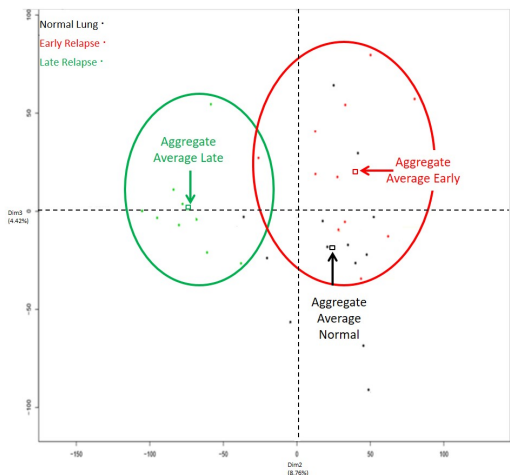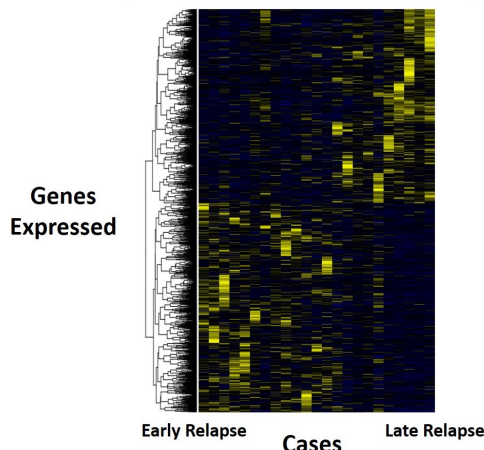Segregates Early/Late Relapse and Normal Lung

Figure 2 - 927

Differential Expression Gene Analysis Heatmap

Conclusions: The results of this study show that upstream regulators including oncogenes and transcriptional regulators are significantly activated in patients with early relapse with EGFR TKIs. Additionally, *MDK, CDC20,* and *GRHL1* were found to have significantly increased expression in early and late relapse. These findings may allow us to predict which patients may benefit from EGFR TKIs with a long term response and which ones may benefit from alternative therapies. Furthermore, *TGFB and PIK3CA* inhibitors may provide an alternate actionable therapeutic pathway in early relapse.

928 Lepidic-Like Pattern of Metastasis in Solitary Pulmonary Nodules: A Systematic Review with Radiologic-Pathologic Correlation of a Deceptive Phenomenon

Jose Manuel Gutierrez Amezcua[1], Fang Zhou[2], Leah Azour[3], Navneet Narula[3], Andre Moreira[3], Esther Adler[3]
[1]New York University Medical Center, New York, NY, [2]NYU School of Medicine, New York, NY, [3]NYU Langone Health, New York, NY

Disclosures: Jose Manuel Gutierrez Amezcua: None; Fang Zhou: None; Navneet Narula: None; Andre Moreira: None; Esther Adler: None

Background: Subsolid nodules (SSNs) represent a diverse range of pulmonary lesions, including various benign and malignant etiologies, the latter most commonly in the spectrum of invasive lung adenocarcinoma with lepidic components. Neoplastic SSNs can rarely represent metastases from extrapulmonary malignancies, with case reports of metastases with lepidic-like growth pattern. To date, however, no systematic review exists describing the frequency of this presentation for metastasis, and their radiologic-pathologic correlation.

Design: We conducted a single-institution retrospective analysis to identify all cases of solitary pulmonary metastasis accessioned between January 2016 and May 2020. Pathology slides and radiology imaging were retrieved and evaluated to assess the frequency of pulmonary metastasis with lepidic-like pattern, and their radiological correlate.

Results: From a total of 77 cases, ten (13%) had varying degree of lepidic-like pattern on histological evaluation, divided into minimal (<5 %; n=5) and significant (> 30%; n=5). The cases with minimal lepidic component had solid (n=3), subsolid (n=1) and cystic (n=1) attenuation on high-resolution CT, whereas those with significant lepidic component were subsolid (n=4) and cavitary (n=1). These metastases originated from melanoma (n= 3) and GI malignancies (n=7; colorectal: 3, pancreatic: 3 and gastroesophageal :1). No statistically significant difference was found in the interval between primary cancer diagnosis and pulmonary metastasis (37.5 vs 46.6 months, *p*= 0.41) or nodule size (1.4 vs 1.6 cm, *p*=0.54) depending on the presence or absence of lepidic component.

Table 1: Radiological Features of Metastases Presenting as Solitary Pulmonary Nodules

Pattern of growth	Non-Lepidic (n=67)	Lepidic (n=10)
Attenuation	Solid (89.5%), Predominantly Solid* (4.5%), Mixed (3%), SSN* (1.5%), Cystic (1.5%)	Minimal (n=5): Solid (60%), SSN (20%), Cystic (20%) Significant (n=5): SSN (80%), Cavitary (20%)
Interval of primary cancer to metastasis	46.6 months (0 – 288)	37.5 months (3 – 480)
Nodule Size (cm)	1.6 (0.8 – 2.3)	1.4 (0.7 – 3)
Wedge resection	25 (37.3%)	5 (50%)
Segmentectomy	7 (10.4%)	2 (20%)
Lobectomy	8 (11.9%)	2 (20%)
Percutaneous biopsy	24 (35.8%)	1 (10%)
Transbronchial biopsy	3 (4.6%)	0

* Three cases had subsolid appearance on imaging but only a biopsy was performed. Possible lepidic components could be missed since the more solid portions are targeted.

Abbreviations: SSN=Subsolid Nodule

Figure 1 - 928
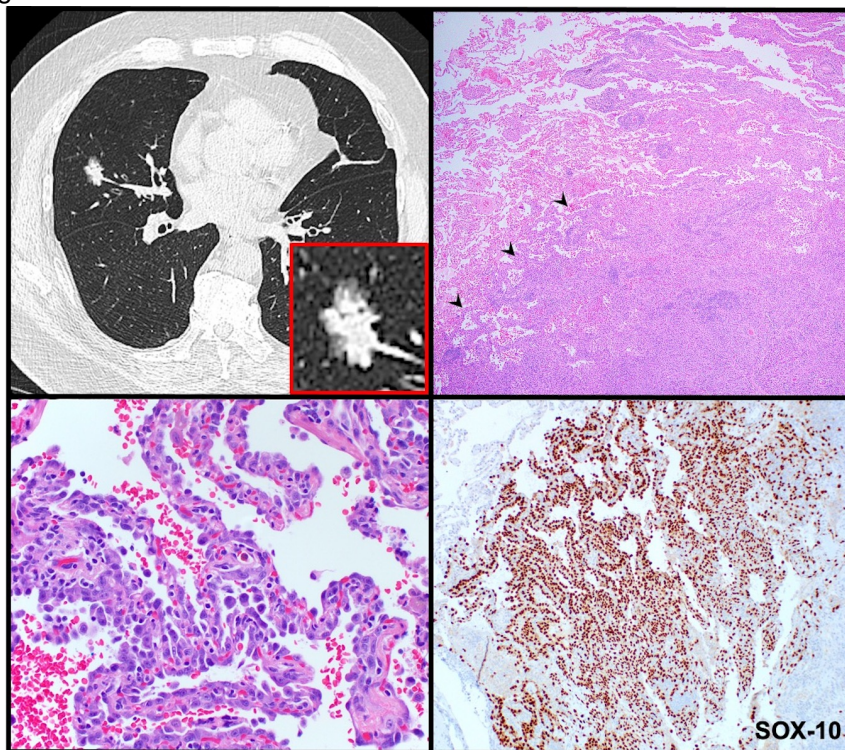
Conclusions: We present, to the best of our knowledge, the first retrospective case series analysis of solitary pulmonary metastasis with lepidic-like pattern and radiologic-pathologic correlation. Similar to previous case reports, most cases with significant lepidic component present as SSNs and they are more commonly found in melanoma (Fig. 1), gastrointestinal and pancreaticobiliary malignancies. Although some authors have suggested this pattern might represent an early stage of cancer growth, we found no statistically significant difference in the interval between primary cancer diagnosis and pulmonary metastasis or nodule size on imaging depending on the presence or absence of lepidic component. Recognition of this atypical pattern of metastasis is crucial, as overlap of the clinical and imaging characteristics of SSNs may obfuscate or delay diagnosis.

929   The Impact of Subtyping and Histologic Grading on the Prognosis of Epithelioid Pleural Mesothelioma

Naomi Hardy[1], Stephanie Richards[2], Rachel Fanaroff[3], Melissa Culligan[3], Joseph Friedberg[3], Allen Burke[4]
[1]University of Maryland Medical Center, Baltimore, MD, [2]Jackson Memorial Hospital/University of Miami Hospital, Miami, FL, [3]University of Maryland, Baltimore, MD, [4]University of Maryland Medical School of Medicine, Baltimore, MD

Disclosures: Naomi Hardy: None; Stephanie Richards: None; Rachel Fanaroff: None; Melissa Culligan: None; Joseph Friedberg: None; Allen Burke: None

Background: Grading systems that may have prognostic value have been proposed for epithelioid malignant mesotheliomas. This study compares the efficacy of a pattern subclassification with a 2- and 3-tier grading system to predict overall and recurrence-free survival in patients with pleural mesothelioma.

Design: A retrospective, 5-year review of patients diagnosed with epithelioid type pleural mesothelioma at an academic hospital was performed. Demographics, time to recurrence, and overall survival were stratified by histologic subtype (worst and predominant) including tubulopapillary, trabecular, solid, micropapillary, and pleomorphic patterns. A 2 tier and 3 tier grading scheme were applied to each case, with the 2 tier encompassing grade 1 (nuclear grade 1, or 2 without necrosis) or 2 (nuclear grade 2 with necrosis, or grade 3); the 3 tier was calculated as follows: nuclear atypia 1=mild, 2=moderate, 3=severe and mitotic score 1=<1/10 HPF, 2=2-4/10 HPF, 3=>5/10 HPF (sum 2 or 3 = grade 1, 4 or 5= grade 2, and 6 = grade 3). Overall and recurrence-free survival was evaluated using a Kaplan-Meier analysis stratified by grade and epithelioid type, with differences between groups analyzed via chi-square, log rank tests.

Results: 42 cases were identified with follow-up data. By histologic pattern, pleomorphic, micropapillary, and trabecular had worse recurrence-free survival compared to solid and tubulopapillary (p=0.004, Figure 1). Pleomorphic and solid type patterns had significantly higher grade compared to trabecular, tubulopapillary and micropapillary (p<0.001). Neither the 2 nor the 3 tier grading systems showed a significant prognostic difference between tiers for overall survival; however, the 3 tier grading system did prognosticate between tiers in terms of extrathoracic recurrence-free survival (p=0.04, Figure 2).
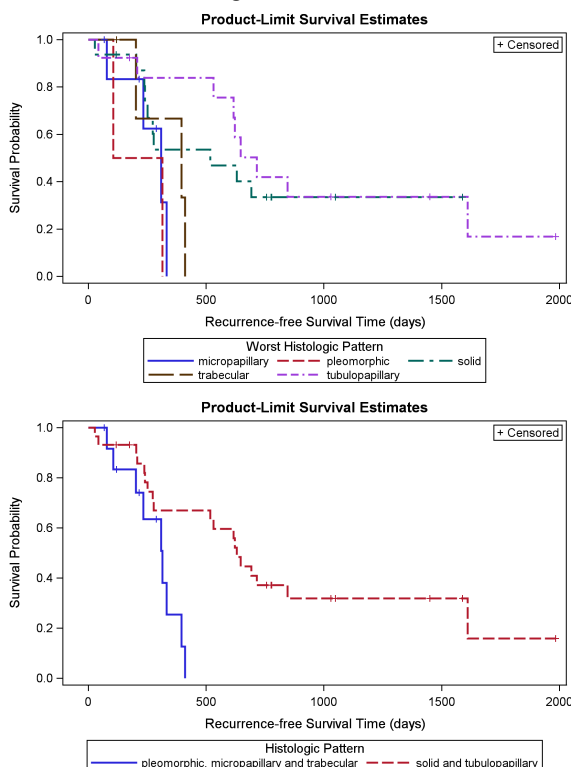
Figure 1 - 929

Figure 2 - 929
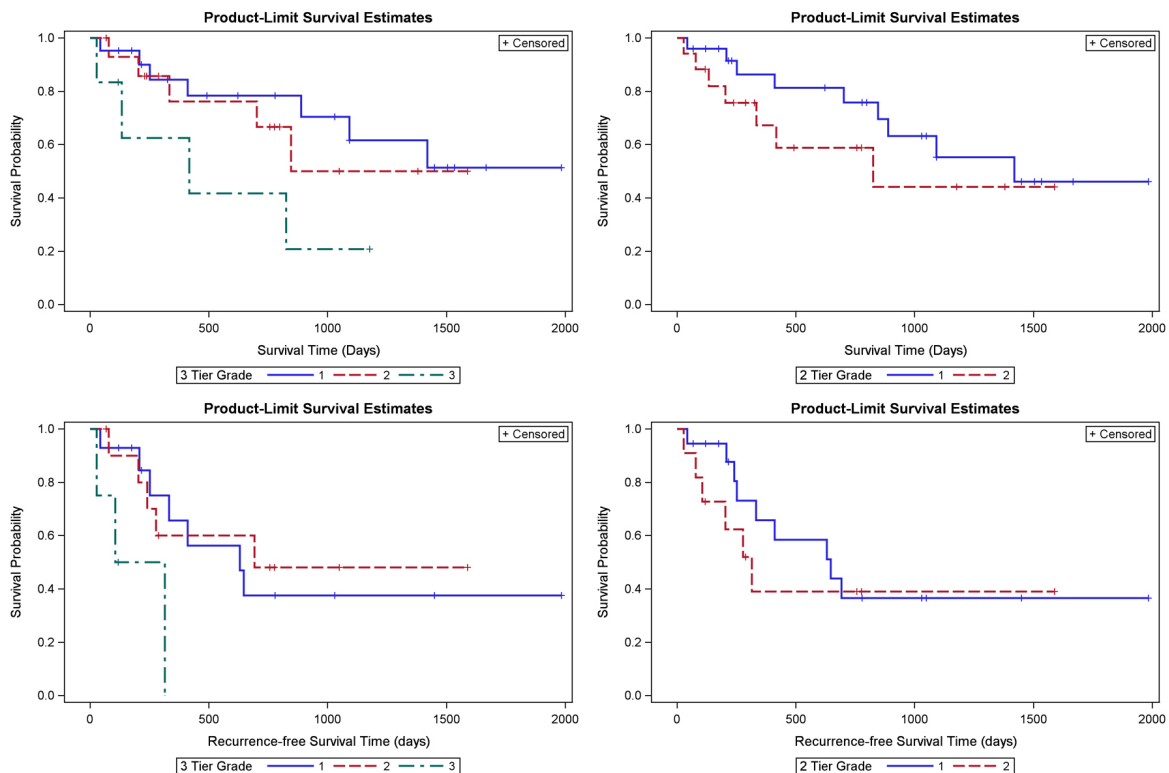
Conclusions: Although there is a good correlation between histologic grade and increasing aggressive subtype, two patterns that were found to have a poor prognosis (trabecular and micropapillary) had relatively low grade. This finding may explain the only moderate correlation between grade and prognosis. A grading system incorporating both pattern as well as cytologic features may provide more accurate prognostication.

930   Optical Imaging for Rapid, Volumetric Assessment of Tumor Adequacy in Lung Core Needle Biopsy

Timothy Helland[1], Sreyankar Nandy[1], Benjamin Roop[1], Rebecca A. Israel[1], Amy Ly[1], Madelyn Lew[2], Anastasia Sorokina[3], Margit Szabari[1], Sarita Berigei[1], David Adams[1], Florian Fintelmann[1], Melissa Suter[1], Lida Hariri[4]
[1]Massachusetts General Hospital, Boston, MA, [2]University of Michigan, Ann Arbor, MI, [3]Research Institution of Human Morphology, Moscow, Russia, [4]Massachusetts General Hospital, Harvard Medical School, Boston, MA

Disclosures: Timothy Helland: None; Sreyankar Nandy: None; Benjamin Roop: None; Rebecca A. Israel: None; Amy Ly: None; Madelyn Lew: None; Anastasia Sorokina: None; Margit Szabari: None; Sarita Berigei: None; David Adams: None; Florian Fintelmann: None; Melissa Suter: *Primary Investigator*, NinePoint Medical; Lida Hariri: None

Background: The ability to make accurate histologic diagnoses, send tissue for molecular testing and bank tumor for future research all hinge on the adequacy of samples obtained with core-needle biopsies (CNB). The use of CT guidance has allowed more accurate procurement of lesional tissue, but cases in which a sub-optimal amount of tumor is sampled remain common. One of the confounding variables is tumor associated fibrosis, which can contaminate CNB and reduce tumor yield. Currently, there is no method in standard use for rapid and non-destructive intraprocedural assessment of CNB adequacy. Polarization-sensitive optical coherence tomography (PS-OCT) is a high-resolution, volumetric imaging technique that could be a valuable tool in intra-operative CNB adequacy evaluation. PS-OCT detects endogenous tissue contrast related to birefringence and depolarization, and can be utilized to provide rapid, label-free, non-destructive, volumetric assessment of tumor yield.

Design: This study included 42 fresh intact CNBs that were obtained from 8 different patients (five male; three female). The mean age of the patients was 72 years (range 51-83). The lung CNB specimens were first imaged with PS-OCT and then submitted for histology with hematoxylin and eosinophil and trichrome stains. Tumor, fibrosis, and normal lung parenchyma content was quantified for each CNB on PS-OCT and histology and compared in a blinded, independent assessment.

Results: Linear regression analysis showed strong correlations between PS-OCT and matched histology for quantification of tumor (r=0.84, p <0.001), fibrosis (r=0.89, p <0.001), and normal lung parenchyma (r=0.86 p <0.001) in CNB specimens. PS-OCT accurately classified CNBs with low tumor content (≤25%) from those with higher tumor content (>25%) with a sensitivity and specificity of 94.4% and 83.3%, respectively. CNBs containing low fibrosis (≤25%) were also accurately classified from those with higher fibrosis content (>25%) by PS-OCT with a sensitivity and specificity of 96.9% and 88.9%, respectively.

Figure 1 - 930
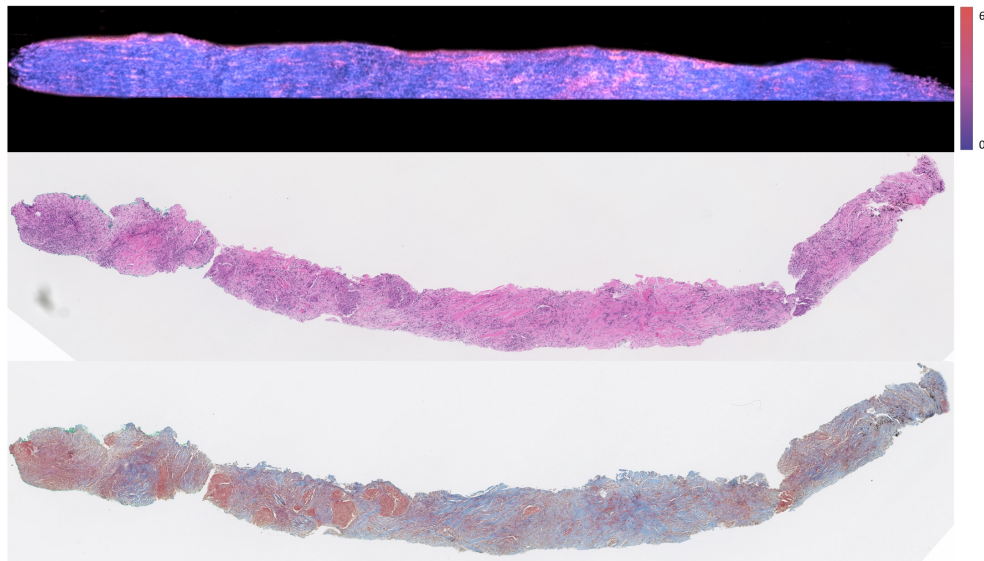
Conclusions: The use of PS-OCT appears to be useful tool in rapidly evaluating the tumor yield in lung CNB. With the ability to distinguish between fibrotic lung and areas involved by tumor, it may employed as a potential method of determining adequacy in the intra-operative setting.

931 Morphologic Classification of Non-Small Cell Carcinoma of Lung Based on a Web-Based Global Survey

Ali Ismail[1], Samer AlQuran[2], Dibson Gondim[1]
[1]University of Louisville, Louisville, KY, [2]University of Louisville Hospital, Louisville, KY

Disclosures: Ali Ismail: None; Samer Al-Quran: None; Dibson Gondim: None

Background: The distinction of primary lung squamous cell carcinoma (SCC) from adenocarcinoma (ADCA) is critical for proper patient management. The diagnostic process starts with evaluation of tumor morphologic features on frozen or permanent sections. The degree of difficulty of solely morphologic distinction ranges from easy to impossible. If there is no certainty, immunohistochemistry is usually the next diagnostic tool used. Given the challenge of defining the spectrum of morphologic diagnostic certainty, we developed a web-application (web app) to answer this question based on a global survey.

Design: Digital slides of cases of SCC and ADCA of lung were randomly selected from The Cancer Genome Atlas (TCGA) project dataset. Each slide was examined, and 1 to 5 areas with viable tumor were selected. Slides with no tumor were excluded. The final dataset consisted of 205 slides of SCC and 243 slides from ADCA. For each selected area, two images equivalent to low- and high-power fields were extracted. A serverless web app that displays each image and has two options for user selection, "SCC" or "ADCA," was deployed to collect the answers. The application shows 40 images per session. The images from each session are randomly chosen from a poll of 1004 images. Usage analytics was collected with google analytics (https://analytics.google.com).

Results: Data were collected for three days after deployment. The web app was used by users from 74 countries, including India (27%), USA (14%) and Brazil (8%). During this period, 14.217 answers were collected. The number of answers per image ranged from 1 to 25 (average 14). The percent of correct answers was calculated for each image. 81/1004 images were correctly answered with 100% agreement between observers. 440/1004 of images were correctly answered with more than 75% agreement. Interestingly, 6/1004 images were incorrectly classified by all the observers; these were images of SCC that were misclassified as ADCA.

Conclusions: Global morphologic survey based on a web app can be used to collect histopathologic interpretation data on a global scale. There are morphologic patterns of non-small cell carcinoma of lung that are correctly and incorrectly classified with a high agreement level. The images on these two extremes could be potentially used as image prototypes to better define the morphologic boundaries of certainty. Future direction is to examine images and identify specific diagnostic criteria from classic cases based on findings of this study.

---

932   Prevalence of High Tumor Mutational Burden in PD-L1 Negative Lung Cancers in a Cohort of 79 Patients Undergoing Comprehensive Genomic Profiling

Nitin Kondapalli[1], Shirley Shiller[2], Pranil Chandra[3]
[1]Baylor University Medical Center, Irving, TX, [2]Baylor University Medical Center, Dallas, TX, [3]Pathgroup, Nashville, TN

Disclosures: Nitin Kondapalli: None; Shirley Shiller: None

Background: Tumor mutational burden (TMB) is the number of somatic mutations present in the genome of tumor cells, typically expressed as the number of mutations per megabase (Mb). TMB received FDA-approval as a pan-tumor biomarker, with greater response to treatment with Pembrolizumab (Immune Checkpoint Inhibitor or ICPI) compared to platinum doublet chemotherapy (KEYNOTE158). High TMB indicates tumor cells undergoing a greater number of mutations which increases immunogenic neoantigen expression on the tumor surface. When neoantigens are recognized by cytotoxic T cells, a strong immune response is elicited, thus indicating a likelihood to respond well to immune-oncology therapy (I-O therapy). Programmed Death Ligand 1 (PD-L1) is a surface protein present on the surface of tumor cells in high number and attaches to the Programmed Death 1 (PD1) protein on T lymphocytes preventing the body's immune system to attack the tumor cells (Immune checkpoint).

Design: Retrospective review of the first 79 cases of lung cancer sequentially received for PGDx elio™ tissue complete/Endeavor testing (FDA cleared) was conducted. This is a 500+ full coding gene sequencing assay that also detects MSI, TMB, and complex alterations: amplifications, translocations. PD-L1 testing is offered by immunohistochemistry using the previously described protocols under the FDA label for Pembrolizumab.

Results: TMB-H occurs in 35% of all lung cancers (NSCLC and SCLC combined) and 34% of NSCLC (29% of adenocarcinomas and 47% of squamous cell carcinoma) in our retrospective review. TMB-H was a qualifying biomarker for Pembrolizumab in 35% of adenocarcinomas and 44% of squamous cell carcinomas of the lung, as these cases were PD-L1 negative. In the SCLC cohort, TMB-H is detected in 100% of tumors.
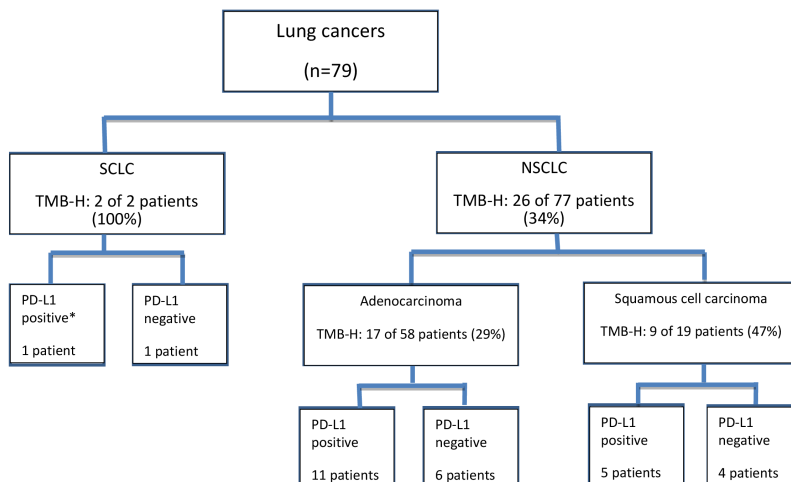
Figure 1 - 932

Figure 1. Overview of study

*CD274 amplification

Abbreviations: NSCLC: Non-small cell lung cancer; PD-L1: Programmed Death Ligand 1; SCLC: Small cell lung cancer; TMB-H : Tumor Mutational Burden- High.

Conclusions: This study defines the prevalence of high TMB (≥16 mutations per Mb for our assay; TMB-H) in our cohort of lung cancers and also highlights the significant number of lung cancers that are negative for PD-L1 by IHC but are TMB-H. Given the significant number of lung cancers that are TMB-H and negative for PD-L1, testing of TMB in these cancers provides an independent biomarker that may qualify patients for FDA-approved for Pembrolizumab therapy upon progression on prior therapy, with no satisfactory treatment options. This study underscores the importance of comprehensive genomic profiling to identify TMB-H patients and highlights its critical role in the genomic profiling workup of patients with advanced lung tumors.

933   Assessment of RICTOR Amplification and mTORC2 Activity in Small Cell Lung Carcinoma: A Comparison of Various Methods

Ildiko Krencz[1], Daniel Sztankovics[1], Titanilla Dankó[1], Noemi Nagy[1], Gábor Petővári[1], Judit Papay[1], Anna Sebestyen[1], Andras Khoor[2]
[1]Semmelweis University, Budapest, Hungary, [2]Mayo Clinic, Jacksonville, FL

Disclosures: Ildiko Krencz: None; Daniel Sztankovics: None; Titanilla Dankó: None; Gábor Petővári: None; Anna Sebestyen: None; Andras Khoor: None

Background: Small cell lung carcinoma (SCLC) is characterized by unique genetic alterations, which often involve the mTOR pathway. Amplification of *RICTOR*, an essential component of mTORC2, has recently been identified as the most common targetable molecular alteration in SCLC. Selection of SCLC patients who may benefit from mTOR inhibitor therapy is currently problematic. The goal of our study was to address this issue by comparing various methods available to assess *RICTOR* amplification and mTORC2 activity.

Design: Droplet Digital PCR and fluorescence in situ hybridization (FISH) were used to detect *RICTOR* gene amplification, and immunohistochemistry (IHC) and Western blot analysis were used to assess mTOR pathway protein expression in SCLC cell lines (n=9). FISH for *RICTOR* amplification and IHC for Rictor and p-Akt expression were also performed on SCLC samples (n=100).

Results: *RICTOR* amplification was detected in 2 SCLC cell lines (22%) and 15 SCLC cases (15%). Expression of mTORC2 pathway proteins correlated with *RICTOR* amplification. As compared to *RICTOR* FISH, the sensitivity

and specificity of Rictor IHC for the detection of *RICTOR* amplification was 93% and 73%, respectively. A high negative predictive value (98%) was also observed.

Conclusions: Our data suggest that *RICTOR* amplification results in Rictor overexpression and mTORC2 hyperactivation in SCLC. Rictor IHC can be used as a cost-effective screening method to select patients for molecular testing and mTOR inhibitor therapy.

934   Extracting Morphological Features to Differentiate Histological Subtypes of Lung Adenocarcinoma: An Attempt to Improve Diagnostic Accuracy by Using a Deep Learning Algorithm

Kris Lami[1], Richard Attanoos[2], Mary Beth Beasley[3], Sabina Berezowska[4], Luka Brcic[5], Alberto Cavazza[6], John English[7], Alexandre Fabro[8], Kaori Ishida[9], Yukio Kashima[10], Brandon Larsen[11], Alberto Marchevsky[12], Anja Roden[13], Frank Schneider[14], Maxwell Smith[11], Kazuhiro Tabata[15], Angela Takano[16], Tomonori Tanaka[17], Andrey Bychkov[18], Junya Fukuoka[19]
[1]Nagasaki University Graduate School of Biomedical Sciences, Nagasaki, Japan, [2]Cardiff University, Cardiff, United Kingdom, [3]Mount Sinai Medical Center, New York, NY, [4]Institute of Pathology, CHUV, Lausanne, Switzerland, [5]Medical University of Graz, Graz, Austria, [6]Azienda USL Reggio Emilia, Reggio Emilia, Italy, [7]Vancouver General Hospital, Vancouver, Canada, [8]Ribeirão Preto Medical School - University of São Paulo, Rio de Janeiro, Brazil, [9]Kansai Medical University, Hirakata, Japan, [10]Awaji Medical Cecter, Awaji, Japan, [11]Mayo Clinic Arizona, Scottsdale, AZ, [12]Cedars-Sinai Medical Center, West Hollywood, CA, [13]Mayo Clinic, Rochester, MN, [14]Emory University, Atlanta, GA, [15]Kagoshima university Graduate School of Medical and Dental Sciences, Kagoshima, Japan, [16]Singapore General Hospital, Singapore, Singapore, [17]Kobe University Hospital, Kobe, Japan, [18]Kameda Medical Center, Kamogawa, Japan, [19]Nagasaki University, Nagasaki-shi, Japan

Disclosures: Kris Lami: None; Richard Attanoos: *Consultant*, APC PATHOLOGY LIMITED; Mary Beth Beasley: None; Sabina Berezowska: None; Luka Brcic: None; Alberto Cavazza: None; John English: None; Alexandre Fabro: None; Kaori Ishida: None; Yukio Kashima: None; Brandon Larsen: *Consultant*, Parexel, Inc.; Alberto Marchevsky: None; Anja Roden: None; Frank Schneider: None; Maxwell Smith: None; Kazuhiro Tabata: None; Angela Takano: None; Tomonori Tanaka: None; Andrey Bychkov: None; Junya Fukuoka: None

Background: Correct recognition of different lung adenocarcinoma (ADC) histologic subtypes is important for prognosis but can be difficult because of similarities between some patterns. Furthermore, there is no clear consensus over the assessment of invasive patterns. The purpose of this study was to find key differences upon the judgment of lung ADC histologic patterns among pathologists to improve diagnostic accuracy by creating a deep learning algorithm.

Design: Twelve surgically resected lung ADC cases encompassing all histologic subtypes were selected. A representative slide from each case was scanned to obtain a whole-slide image (WSI). Each WSI was sliced into 1mm^2 tiles at 5x magnification to obtain 4702 tiles. Eighteen expert pathologists from 9 countries were asked to classify each tile into one subtype of lung ADC. Subtypes included lepidic, acinar, papillary, micropapillary, solid, invasive mucinous, other carcinoma, or no cancer cells.

Results: Among 4702 tiles, 1742 (37%) tiles had an overall consensus among the 18 pathologists, including 1520 tiles labeled as "no cancer cells". Only 4.7% of tiles had a consensus for the lung ADC pattern. The overall Fleiss kappa score for the agreement of all patterns among 18 pathologists was 0.58, while the score for invasive pattern versus non-invasive pattern was 0.66. When separating tiles into invasive and non-invasive, the interobserver agreement had a wide range (0.05-0.76). Example of the case showing wide observer variability is shown in Fig. 1.

Based on results obtained, the pathologists were hierarchically grouped into 3 clusters, mainly based on the difference in the assessment of invasion (Fig. 2). The overall agreement among clusters ranged from 0.59 to

0.66, indicating moderate to substantial agreement. Regarding specific histologic features, pathologists from cluster 1 recognized invasive patterns based on unequivocal signs of stromal invasion, marked cytological atypia, or presence of mucinous contents in the glandular lumen. However, pathologists from cluster 2 rather relied on the presence of a thickened stroma as equivalent to invasion.

Figure 1 - 934
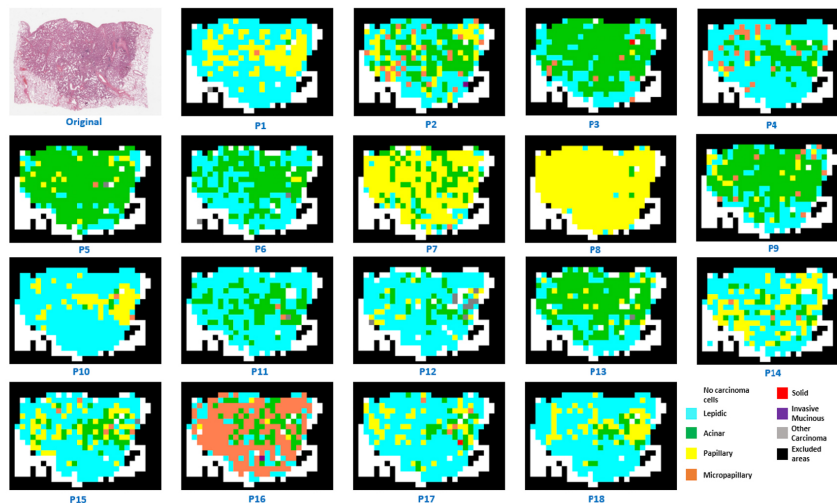
Example of a tile-based heatmap (each color corresponds to the specific histologic pattern) for a single case showing the variability of patterns recognized by different pathologists

Figure 2 - 934
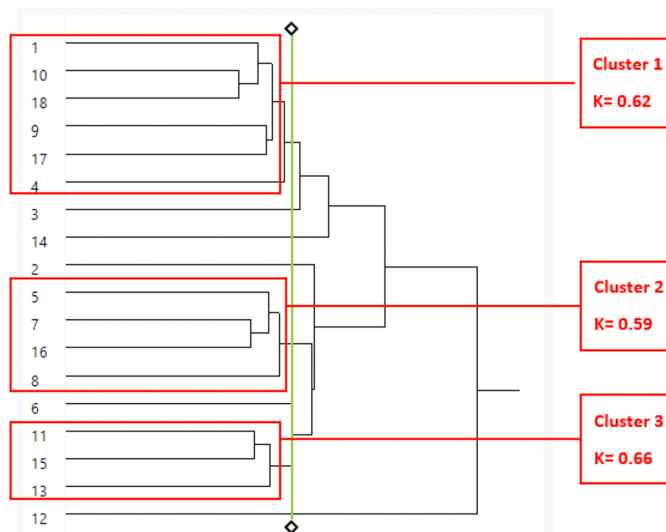
Hierarchical clustering of 18 expert lung pathologists

Conclusions: Our observations highlight discrepancies among clusters of pathologists when assessing subtypes of lung ADC and when judging an image as invasive versus non-invasive. Consensus tiles from each cluster are currently being used as ground truth to train deep convolutional neural networks (CNNs). These CNNs will be competing against each other to predict survival in a large-scale cohort.

935   Utility of Dual YAP/TAZ-NF2 Immunohistochemistry in the Diagnosis of Malignant Pleural Mesothelioma and in Predicting NF2 Mutations

Yan Li[1], Ying-Bei Chen[1], Marjorie Zauderer[1], Jason Chang[1], Michael Offin[1], Marc Ladanyi[1], Natasha Rekhtman[1], William Travis[1], Soo-Ryum Yang[1], Prasad Adusumilli[1], Jennifer Sauter[1]
[1]Memorial Sloan Kettering Cancer Center, New York, NY

Disclosures: YAN LI: None; Ying-Bei Chen: None; Marjorie Zauderer: None; Jason Chang: None; Michael Offin: None; Marc Ladanyi: None; Natasha Rekhtman: None; William Travis: None; Soo-Ryum Yang: None; Prasad Adusumilli: None; Jennifer Sauter: None

Background: TCGA reported neurofibromatosis type 2 (*NF2*) loss in 40% of malignant pleural mesothelioma (MPM). Inactivation of *NF2* can activate the Hippo pathway leading to accumulation of two main downstream effectors, Yes associated protein (YAP) and transcriptional activator with PDZ-binding domain (TAZ) in tumor nuclei. Immunohistochemistry (IHC) for YAP/TAZ and NF2 may be helpful diagnostically in differentiating reactive mesothelial proliferations from MPM. Since *NF2* represents a potential therapeutic target, correlation between NF2 expression by IHC and underlying molecular findings is of clinical value.

Design: YAP/TAZ-NF2 dual IHC (D24E4 and D3S3W, respectively, Cell Signaling Technology) was performed on FFPE from 20 MPM (10 with *NF2* alterations detected by next generation sequencing (NGS) (Table 1) and 10 with no *NF2* alterations; 2 epithelioid (E) and 8 biphasic (B) and 9 E and 1 B, respectively) and 9 cases of benign pleura from patients without MPM. H scores were determined for YAP/TAZ nuclear immunoreactivity. NF2 cytoplasmic and/or membranous immunoreactivity was scored as follows: 0, no staining; 1, <10% of MPM cells; 2, 10-50%; and 3, >50%. Specificity of loss of NF2 immunoreactivity (defined as score < 2) was determined. T-tests were used to compare H-scores.

Results: All 10 *NF2*-altered MPMs showed loss of NF2 immunoreactivity by IHC, while NF2 expression was retained in all MPM without *NF2* alterations and in all benign pleura cases (Table 1). *NF2*-altered MPM were associated with higher YAP/TAZ H-scores compared to MPM without *NF2* alterations (mean 232.5 and 118.5, respectively, $p<0.001$) (Figure 1). *NF2*-wildtype MPM demonstrated moderate nuclear YAP/TAZ immunoreactivity (mean H-score 118.5) compared to benign pleura (mean H-score 21.1, $p<0.001$). Loss of NF2 expression by IHC yielded 100% specificity in differentiating MPM from benign pleura.

Case No	Histology	*NF2* alteration
1	Biphasic	(NM_000268) exon5 p.G161X (c.481G>T)
2	Biphasic	(NM_000268) exon1 splicing variant (c.114+2T>A)
3	Biphasic	(NM_000268) exon8 p. L239fs (c.715delC)
4	Biphasic	(NM_000268) exon2 p. F62Lfs*61 (c.183delC); (NM_000268) - rearrangement: c.109:NF2_chr22: g.30109685del
5	Biphasic	(NM_000268) exon1 p.E34* (c.100G>T)
6	Epithelioid	(NM_000268 - 22q12.2) Deletion (Fold Change: -2.6)
7	Epithelioid	(NM_000268) exon4 splicing variant p.X122_splice (c.364-2A>C)
8	Biphasic	(NM_000268) exon2 p.W41* (c.123G>A)
9	Biphasic	(NM_000268) exon9 p. K289Sfs*7 (c.866delA)
10	Biphasic	(NM_000268 - 22q12.2) Intragenic deletion

Figure 1 - 935

	YAP nuclear H-score (mean ± SD)	NF2 membranous/cytoplasmic score (mean ± SD)
Mesothelioma		
NF2-altered	232.5 ± 27.5	0.30 ± 0.48
NF2-wild type	118.5 ± 57.6	2.70 ± 0.48
Benign pleura	21.1 ± 24.3	2.90 ± 0.33

*Next generation sequencing was used for detection of *NF2* alterations

Conclusions: Loss of NF2 expression by IHC corresponded to detection of *NF2* alterations by NGS. While YAP/TAZ activation was highest in *NF2*-altered MPM, moderate activation was also seen in *NF2*-wildtype MPM, but not in benign pleura. Given its high specificity, NF2 IHC may have diagnostic utility in distinguishing MPM from benign mesothelial proliferations and may also have therapeutic implications as a biomarker for detecting *NF2* alterations in MPM. These results need to be confirmed in larger cohorts.

936   Immunohistochemical Assessments of ALK Protein and its Phosphorylation Site Y1507 Modification Among ALK Gene Fusion Positive Lung Cancers

Rahul Mannan[1], Seema Chugh[2], Xiaoming (Mindy) Wang[2], Anya Chinnaiyan[3], Roshni Rangaswamy[4], Sylvia Zelenka-Wang[3], Xuhong Cao[2], Liron Pantanowitz[2], Jeffrey Myers[5], Tao Huang[2], Arul Chinnaiyan[2], Noah Brown[2], Saravana Dhanasekaran[2], Rohit Mehra[2]
[1]Michigan Medicine, University of Michigan, Ann Arbor, MI, [2]University of Michigan, Ann Arbor, MI, [3]Michigan Center for Translational Pathology, Ann Arbor, MI, [4]Michigan Center for Translational Pathology, Ypsilanti, MI, [5]Michigan Medicine, Ann Arbor, MI

Disclosures: Rahul Mannan: None; Seema Chugh: None; Xiaoming (Mindy) Wang: None; Anya Chinnaiyan: None; Roshni Rangaswamy: None; Sylvia Zelenka-Wang: None; Xuhong Cao: None; Liron Pantanowitz: None; Jeffrey Myers: None; Tao Huang: None; Arul Chinnaiyan: None; Noah Brown: None; Saravana Dhanasekaran: None; Rohit Mehra: None

Background: The *ALK* (Anaplastic Lymphoma Kinase) gene encodes a receptor tyrosine kinase with oncogenic rearrangements in 3-5% of non-small-cell lung cancer (NSCLC). Studies in NSCLC have identified more than 19 different ALK fusion partners such as *EML4*, *KIF5B*, *KLC1*, and *TPR*. Our recent proteogenomic characterization of lung adenocarcinoma cohort identified a consistent increase in ALK protein and specifically ALK phosphosite Y1507 (pALK-Y1507) modification among *ALK* gene fusion positive patient tissue samples. The utility of assaying this ALK phosphosite modification in tissue specimens both as a read out of the functionality of the driver gene fusion and its potential to monitor therapeutic response to ALK inhibitors encouraged the current investigation.

Design: To evaluate the clinical association of pALK-Y1507 modification with ALK driver gene fusion status, total ALK expression and the amount of pALK-Y1507 modification were evaluated in a predominant lung cancer cohort (n=29). The study samples include two different cohorts that comprise a proteogenomically characterized discovery set (n=9; 5 fusion positive and 4 negative) and an independent validation set (n=20; all fusion positive) **Table 1**. Gene fusion status verified samples represent both primary and metastatic disease. Immunohistochemistry (IHC) was performed on tumor, benign and negative control samples with both ALK (D3F5) and pALK-Y1507 (D6F1V) antibodies. Antibody specificity was assessed by transient knockdown of ALK in EML4-ALK fusion positive lung cancer cells (H2228). The staining was quantitated using a scoring method by accounting for percentage

positivity along with staining intensity. A final derived product score was used to evaluate the diagnostic utility of the ALK protein versus Phospho-ALK staining.

Results: Transient knockdown of ALK in H2228 cells confirmed specificity of both ALK (D3F5) and pALK-Y1507 (D6F1V) antibodies. IHC analysis revealed strong to moderate cytoplasmic immune-positive signal for both ALK and pALK-Y1507 (D6F1V) antibodies in our cohort. We observed upregulation of both total ALK and pALK Y1507 specifically in the tumor epithelial component in the majority of *EML4-ALK* fusion-positive samples (90%; 18/20 cases), with no staining observed in matched normal adjacent and benign tissue. For non-*EML4-ALK* fusion cases expression of phospho-ALK was seen in half of the cases (2/4 cases), while all non-*ALK* fusion cases (*ROS* and *RET* fusion) showed no expression of total ALK and pALK-Y1507.

Table-1: Summary of ALK (D3F5) and pALK-Y1507 (D6F1V) IHC score												
EML4-ALK Fusion Cases						S.No	Site	Fusion	Total-ALK*	Phospho-ALK**	Interpretation
S.No	Site	Fusion	Total-ALK*	Phospho-ALK**	Interpretation	16	Lung	EML4-ALK	190	115	ALK + /P-ALK +
1	Lung	EML4-ALK	185	101	ALK + /P-ALK +	17	Lung	EML4-ALK	178	132	ALK + /P-ALK +
2	Lung	EML4-ALK	250	225	ALK + /P-ALK +	18	Lung	EML4-ALK	176	168	ALK + /P-ALK +
3	Lung	EML4-ALK	253	238	ALK + /P-ALK +	19	Lung	EML4-ALK	162	103	ALK + /P-ALK +
4	Lung	EML4-ALK	193	115	ALK + /P-ALK +	20	Lung	EML4-ALK	268	180	ALK + /P-ALK +
5	Lung	EML4-ALK	268	196	ALK + /P-ALK +	Non EML4-ALK Fusion and Negative Control Cases					
6	Lung	EML4-ALK	190	16	ALK + /P-ALK -	SN	Site	Fusion	Total-ALK*	Phospho-ALK**	Interpretation
7	Lung	EML4-ALK	262	191	ALK + /P-ALK +	1	Lung	ANKRD36B-ALK	285	195	ALK + /P-ALK +
8	Lung	EML4-ALK	192	169	ALK + /P-ALK +	2	Renal	TPM3-ALK	218	75	ALK + /P-ALK +
9	Lung	EML4-ALK	142	211	ALK + /P-ALK +	3	Lung	KLC1-ALK	200	25	ALK + /P-ALK +
10	Lung	EML4-ALK	173	162	ALK + /P-ALK +	4	Lung	HIP1-ALK	280	144	ALK + /P-ALK +
11	Lung	EML4-ALK	197	203	ALK + /P-ALK +	5	Colon	STRN-ALK	245	2	ALK + /P-ALK -
12	Lung	EML4-ALK	184	0	ALK + /P-ALK -	6	Lung	ROS1	0	0	Negative Control
13	Lung	EML4-ALK	295	292	ALK + /P-ALK +	7	Lung	RET	0	0	Negative Control
14	Lung	EML4-ALK	233	256	ALK + /P-ALK +	8	Lung	RET	0	0	Negative Control
15	Lung	EML4-ALK	246	267	ALK + /P-ALK +	9	Lung	ROS1	0	0	Negative Control
*- Total-ALK[D3F5] product score; **-Phospho-ALK[Y1507] product score; S.No- Serial number											

Conclusions: This study indicated increased expression of ALK phosphosite Y1507 in *ALK* fusion positive NSCLC cases. These results can be extended to a larger cohort in order to determine the potential utility of these novel biomarker used for diagnosis and to evaluate therapeutic efficacy of ALK inhibitors in *ALK* gene fusion positive lung cancer.

937   Interstitial Megakaryocytes are Associated with Alloantibodies and may be Indicative of Antibody Mediated Rejection in Lung Transplant Recipients

Janina Markidan[1], Rachel Fanaroff[2], Allen Burke[3]
[1]University of Maryland Medical Center, Baltimore, MD, [2]University of Maryland, Baltimore, MD, [3]University of Maryland Medical School of Medicine, Baltimore, MD

Disclosures: Janina Markidan: None; Rachel Fanaroff: None; Allen Burke: None

Background: Interstitial megakaryocytes (IM) have been associated with antibody mediated rejection (AMR). We reviewed a series of surveillance lung transplant biopsies to determine the incidence of IM and the association with clinical findings and alloimmunity.

Design: A 4-year retrospective review was performed of consecutive biopsies, including all lung transplant recipients with 3 or more biopsies and serologic testing. The biopsy slides were reviewed for presence and type of interstitial inflammation and presence of megakaryocytes. The results of the biopsies were correlated with concomitant serologic testing (percent panel reactive antibodies (PRA) and the presence of allele-specific donor antibodies (DSA)), histologic evidence of cellular rejection, presence of acute lung injury (ALI), and clinical findings of rejection, pneumonia, ALI associated with chronic lung allograft dysfunction (CLAD), and systemic infection.

Results: There were 117 patients, 67 men and 50 women, mean age 62 years. There were a total of 537 biopsies reviewed. The patients were divided into those with at least one biopsy showing megakaryocytes (group A, 46 patients) and those with no biopsies showing megakaryocytes (group B, 71 patients).

Clinically, 30 (65%) group A patients had positive DSA. Of these patients, the mean PRA level was 42%, 12 (26%) patients had acute cellular rejection (ACR), 4 (9%) had AMR, 3 (7%) had ALI, and 8 (17%) had pneumonia or systemic infection. In biopsy findings, 10 (22%) group A patients had ACR, 23 (50%) had interstitial neutrophils and macrophages, and 5 (11%) had ALI. Of 16 group A patients who had biopsies with IM and negative DSA, 4 (25%) had ALI/CLAD, 7 (44%) had clinical pneumonitis, 1 (6%) had urosepsis, and 5 (31%) had ACR. Of these 16 patients, 6 (38%) also had non-allele specific DSA. Of 8 group A patients who had biopsies without other interstitial inflammation, 7 (88%) had positive DSA, and one (13%) had non-allele specific DSA. One of these patients also developed recurrent clinical AMR, and one subsequently developed ACR.

Clinically, 2 (3%) patients in group B had positive DSA. Of these patients, the mean PRA level was 13%. 2 patients had ACR, 4 (6%) had pneumonia or systemic infection, and none had AMR or ALI. In biopsy findings, 7 (10%) group B patients had ACR, 7 had interstitial neutrophils and macrophages, and 4 (6%) had ALI.

	Parameter	Positive association, p-value megakaryocytes (group A) v. no megakaryocytes (group B)
Clinical	Presence of DSA	<0.0001
	Mean PRA	<0.0001
	Clinical ACR	<0.0001
	ALI due to PGD/CLAD	0.02
	Pneumonia/ infection	0.02
Pathologic	Pathologic ACR	<0.001
	Interstitial neutrophils and macrophages	<0.0001
	Acute lung injury	0.08

Conclusions: The majority of biopsies with interstitial megakaryocyte occur in patients with donor specific alloantibodies, many of whom have a diagnosis of rejection. They may also be seen in acute lung injury due to infections, and chronic lung allograft dysfunction.

938   Clinicopathologic Characteristics of ARID1A Deficient Non-Small Cell Lung Carcinomas
Daniel Martinez Coconubo[1], Humberto Trejo Bittar[1], Samuel Yousem[1]
[1]University of Pittsburgh Medical Center, Pittsburgh, PA

Disclosures: Daniel Martinez Coconubo: None; Humberto Trejo Bittar: *Consultant*, Unity Biotechnology; Samuel Yousem: None

Background: The *ARID1A* gene (AT-Rich Interaction Domain 1A) encodes a protein that makes part of the SWI/SNF chromatin-remodeling complex. The loss of different components of this protein complex has been associated with a "rhabdoid" morphology across different tumor types. Recently, ARID1A mutations have been found in 7% of lung adenocarcinomas. Furthermore, ARID1A deficient tumors have been shown to be responsive to immune checkpoint inhibitors and *ATR* and *EZH2* inhibitors. The purpose of this study was to assess the histopathologic characteristics and immunohistochemical (IHC) expression of ARID1A in NSCLCs with *ARID1A* next-generation sequencing (NGS) proven mutations.

Design: Nine cases of NSCLCs with *ARID1A* mutations detected by NGS between 2019 and 2020 were identified. We assessed the tumors' histopathologic features and reviewed the patient's demographic characteristics. Tumors were stained for ARID1A with the monoclonal antibody clone EPR13501. Staining was performed on a Ventana Benchmark Ultra with an antibody dilution of 1:500. Tumors were classified into four categories based on the pattern of staining (see figure 1)

Results: Nine cases were identified. The mean patient age was 65 years (*SD*: 8.6). All patients had a prior smoking history. All cases were adenocarcinomas; eight showed poorly differentiated areas, seven showed a giant cell component, and six displayed focal rhabdoid features. Seven cases had nonsense mutations, and 2 had point mutations of *ARID1A*. Six cases with truncating *ARID1A* mutations revealed altered ARID1A immunohistochemical expression. Patterns of altered ARID1A expression included complete diffuse loss (1), diffuse decreased expression (2) complete but heterogeneous loss (2), and heterogeneous decreased expression (1). One case with ARID1A variant p.R1383W had retained ARID1A expression by immunohistochemistry; this case had copy number loss of the 19p region (SMARCA4) and showed corresponding complete loss of SMARC4A by immunohistochemistry. A case with *ARID1A* variant p. K1677* demonstrated retained ARID1A IHC expression.

Figure 1 - 938
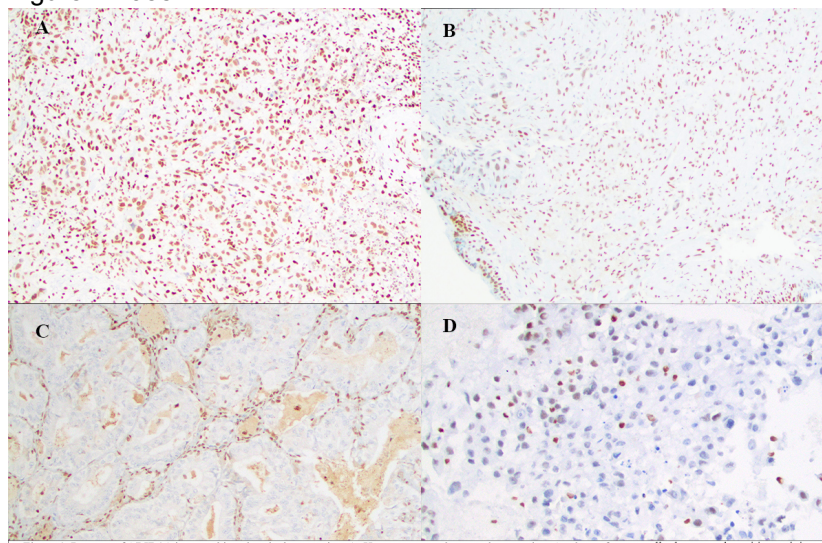
Figure 1. Patterns of ARID1A immunohistochemical expression. A: Heterogeneous decreased expression. A subset of tumor cells shows weak positive staining compared to a subset of strongly positive tumor cells. B: Diffuse decreased expression. All tumor cells are weakly positive compared to background inflammatory cells. C: Diffuse complete loss. All tumor cells are negative, with positive background inflammatory cells. D: Heterogeneous complete loss. A portion of tumor cells shows negative staining with some strongly positive tumor cells present.

Conclusions: NSCLCs with *ARID1A* mutations tend to be poorly differentiated adenocarcinomas with giant cell and rhabdoid features. Tumors with nonsense mutations of *ARID1A* tend to show altered ARID1A immunohistochemical expression; however, staining patterns are heterogeneous, including completely retained expression. Screening of poorly-differentiated NSCLCs for *ARID1A* mutations by immunohistochemistry might not be sufficiently accurate.

939   Genomic Landscape of Pleural Mesotheliomas (PMs) Based on Genomic Loss of Methylthioadenosine Phosphorylase (MTAP)

Douglas Mata[1], Stephanie Bryant[2], Tyler Janovitz[1], Brennan Decker[1], Richard Huang[3], Douglas Lin[1], J. Keith Killian[1], Shakti Ramkissoon[4], Ole Gjoerup[1], Natalie Danziger[1], Jeffrey Ross[2]
[1]Foundation Medicine, Inc., Cambridge, MA, [2]SUNY Upstate Medical University, Syracuse, NY, [3]Foundation Medicine, Inc., Cary, NC, [4]Foundation Medicine, Inc., Morrisville, NC

Disclosures: Douglas Mata: *Employee*, Foundation Medicine, Inc.; Stephanie Bryant: None; Tyler Janovitz: *Employee*, Foundation Medicine; Brennan Decker: *Employee*, Foundation Medicine; Richard Huang: *Employee*, Foundation medicine; Douglas Lin: *Employee*, Foundation Medicine, Inc.; *Stock Ownership*, Roche; J. Keith Killian: *Employee*, Foundation Medicine; Shakti Ramkissoon: *Employee*, Foundation Medicine; Ole Gjoerup: None; Natalie Danziger: *Employee*, Foundation Medicine Inc.; Jeffrey Ross: *Employee*, Foundation Medicine; *Advisory Board Member*, Tango Therapeutics

Background: PMs are aggressive malignancies with limited therapy options in the unresectable or metastatic disease setting. Emerging treatment strategies for clinically advanced PMs include immune checkpoint inhibitors (ICPIs) and novel synthetic lethality agents that target protein arginine methyl transferases (e.g., PRMT5), exploiting the impact of genomic loss of *MTAP*.

Design: Of 140,182 cases of clinically advanced and metastatic cancers submitted for hybrid capture-based comprehensive genomic profiling (CGP), 0.3% (361) were PMs and included in this study. Tumor mutational burden (TMB) was determined on up to 1.1 Mb of sequenced DNA and microsatellite instability (MSI) was determined on 114 loci. PD-L1 expression was determined by IHC (Dako 22C3).

Results: In all, 33% (119/361) of the PMs exhibited *MTAP* deletion, the majority of which had concurrent deletion of *CDKN2A* (99.2%) and *CDKN2B* (93.3%) at 9p21. PMs with *MTAP* deletion were more likely to harbor alterations in *NF2* (43.7% vs. 31.0%, P=0.02) and less likely to harbor alterations in *TP53* (14.3% vs. 24.4%, P=0.03) or *SETD2* (0.8% vs. 15.7%, P=0.004) than were those that were *MTAP* intact. *BAP1* alteration frequencies were similar in both groups (46.2% vs. 45.9%, P=1.0). Biomarkers potentially impacting ICPI such as TMB and MSI status were similarly low in the *MTAP*-deleted and *MTAP*-intact groups. PD-L1 low-positive expression was near 50% in both groups; however, PD-L1 high-positive expression was more frequent in PMs with loss of *MTAP* (20 vs. 7%, P=0.03). Genetic alterations (GAs) in *PBRM1*, which may predict ICPI efficacy, were less frequent in *MTAP*-deleted PMs (1.7% vs. 9.5%, P=0.01). GAs in genes associated with PARP inhibitor efficacy, including *BRCA2*, were infrequent in both groups.

	MTAP-deleted PM (n = 119)	*MTAP*-intact PM (n = 242)	Significance
Males/Females	79%/21%	66%/34%	P=0.01
Median age (range), years	74 (46-89+)	73 (30-89+)	NS
NF2	52 (43.7%)	75 (31.0%)	P=0.02
BAP1	55 (46.2%)	111 (45.9%)	NS
CDKN2A	118 (99.2%)	64 (26.4%)	P<0.0001
CDKN2B	111 (93.3%)	48 (19.8%)	P<0.0001
TP53	17 (14.3%)	59 (24.4%)	P=0.03
SETD2	1 (0.8%)	38 (15.7%)	P=0.004
PBRM1	2 (1.7%)	23 (9.5%)	P=0.01
BRCA2	4 (3.4%)	7 (2.9%)	NS

RAD21	2 (1.7%)	6 (2.5%)	NS
TERT	11 (9.2%)	23 (9.5%)	NS
PTEN	5 (4.2%)	7 (2.9%)	NS
PBRM1	2 (1.7%)	23 (9.5%)	0.01
GAs/tumor	4.2	3.0	NS
Median TMB	1.3	1.3	NS
Mean TMB	2.0	2.1	NS
TMB ≥10 mt/Mb	2%	3%	NS
TMB ≥20 mt/Mb	0%	.4%	NS
MSI High	0 (0%)	1 (0.4%)	NS
PD-L1 Low Positive (1-49%)	28/56 (50.0%)	50/109 (45.9%)	NS
PD-L1 High Positive (≥50%)	11/56 (19.6%)	8/109 (7.3%)	P=0.03

Conclusions: *MTAP* deletion occurred in 33% of PMs and was associated with differing frequencies of GAs in *NF1*, *TP53*, *SETD2*, and *PBRM1*. The comparison of ICPI biomarkers in *MTAP*-deleted and *MTAP*-intact PMs was complicated by the former having higher PD-L1 high-positive expression and the latter having more GAs in *PBRM1*. Further study of anti-PRMT5 drugs that are enabled by *MTAP* loss is warranted.

940   Comparison of DNA and RNA Based Sequencing for Detecting MET exon 14 Skipping Mutations and Their Morphologic Correlate in Patients with Non-Small Cell Lung Cancer
Harshita Mehrotra[1], Kanika Arora[1], Laura Favazza[2], Dhananjay Chitale[2]
[1]Henry Ford Health System, Detroit, MI, [2]Henry Ford Hospital, Detroit, MI

Disclosures: Harshita Mehrotra: None; Kanika Arora: None; Laura Favazza: None; Dhananjay Chitale: None

Background: MET exon 14 skipping alterations (*MET*ex14) are reported in 2-4% of patients with non-small lung cell carcinoma (NSCLC) and provide an attractive therapeutic target. RNA sequencing methods offer a direct evidence of *MET*ex14. In this study, we compare detection of *MET*ex14 NSCLC detected by RNA sequencing with DNA sequencing by using multigene next generation sequencing (NGS) panels.

Design: All NSCLC cases tested for *MET*ex14 alterations from 01/01/2018 to 09/30/2020 were reviewed. Genomic DNA and RNA were extracted using standard protocols for formalin fixed paraffin embedded tissues and cytology cellblocks (minimum 10 ng input DNA and 20 ng RNA). RNA sequencing was performed using Archer Solid Tumor FusionPlex RNA panel that included primers flanking exons 13 through 15 of *MET* gene. Targeted DNA NGS panel included *MET* gene covering exons 2, 14, 16, and 19 exons and partial introns of 13 and 14. Assay acceptability criteria included minimum depth of coverage 200X for RNA and 500X for DNA assays and percent uniformity of coverage >70%. Other RNA panel quality matrix included Reads After Trimming > 2,000,000; Average Unique RNA Start Sites per GSP2 Control >= 10.

Results: Out of 828 cases of NSCLC, 11 were positive for *MET*ex14 skipping (1.3%) detected by RNA sequencing. Representative images of positive tumors are given in figure 1 and patient characteristics are given in figure 2. There were 8/11 (72%) females, median age 76 years (range 58 to 100), 8/11 (72%) Caucasians, 6/11(54.5%) smokers, and 5/11 (45.5%) had metastatic disease at presentation. 8/11 (72%) cases were adenocarcinoma, 2 (18.2%) squamous cell carcinoma, and 1 (9%) poorly differentiated NSCLC. Overall survival ranged from 0 to 18 (average 9.8) months and 5 patients (45.5%) were alive at the time of record review. DNA sequencing showed canonical splice site DNA mutations either at -1 or -2 in 3/11 cases, 2/11 had a mutation in intron 14 at +3, 2/11 cases had known p.Asp1028His hotspot mutation, 1/11 had a novel 3 base-pair deletion at -16 (c.2942-16_2945del), 1/11 case showed a frameshift alteration (currently of uncertain significance) p.Glu1012Asnfs*5, and 2/11 cases showed no DNA alterations. DNA and RNA alterations are given in table 1.

| Case number	Transcript	cDNA Change	Protein Change	Depth of Coverage	Allele Fraction	Corresponding RNA breakpoint
1	NM_001127500	c.2942-16_2945del	20 base pair deletion involving 3' splice site	7384	37.60%	chr7:116411708, chr7:116414935
2	NM_001127500	c.3082+3A>T	Splice donor	3319	21.80%	chr7:116411649, chr7:116411708
3	NM_001127500.1	c.3082G>C	p(Asp1028His)	24657	47.00%	chr7:116411708, chr7:116414935
4	No CODING VARIANTS DETECTED IN MET TARGETED REGIONS TESTED					chr7:116411708, chr7:116414935
5	NM_001127500.1	c.3034_3035delGA	p(Glu1012Asnfs*5)	5410	16.80%	chr7:116411640, chr7:116411708
6	NM_001127500	c.3082+3A>T	Splice donor at 5' site	3319	21.80%	chr7:116411649, chr7:116411708
7	NM_001127500.1	c.3082+1G>C	Splice donor at 5'site	51898	38.00%	chr7:116411708, chr7:116414935
8	NM_001127500.1	c.3082G>C	Splice donor	6969	21.00%	chr7:116411708, chr7:116414935
9	NO CODING VARIANTS DETECTED IN MET TARGETED REGIONS TESTED					chr7:116411708, chr7:116414935
10	NM_001127500.1	c.3082+1G>A	Splice donor at 5' site	18435	42.00%	chr7:116411607, chr7:116411708; chr7:116414935, chr7:116415150
11	NM_001127500.1	c.3082+2T>C	Splice donor at 5' site	38464	16.00%	chr7:116411708, chr7:11641493

Figure 1 - 940
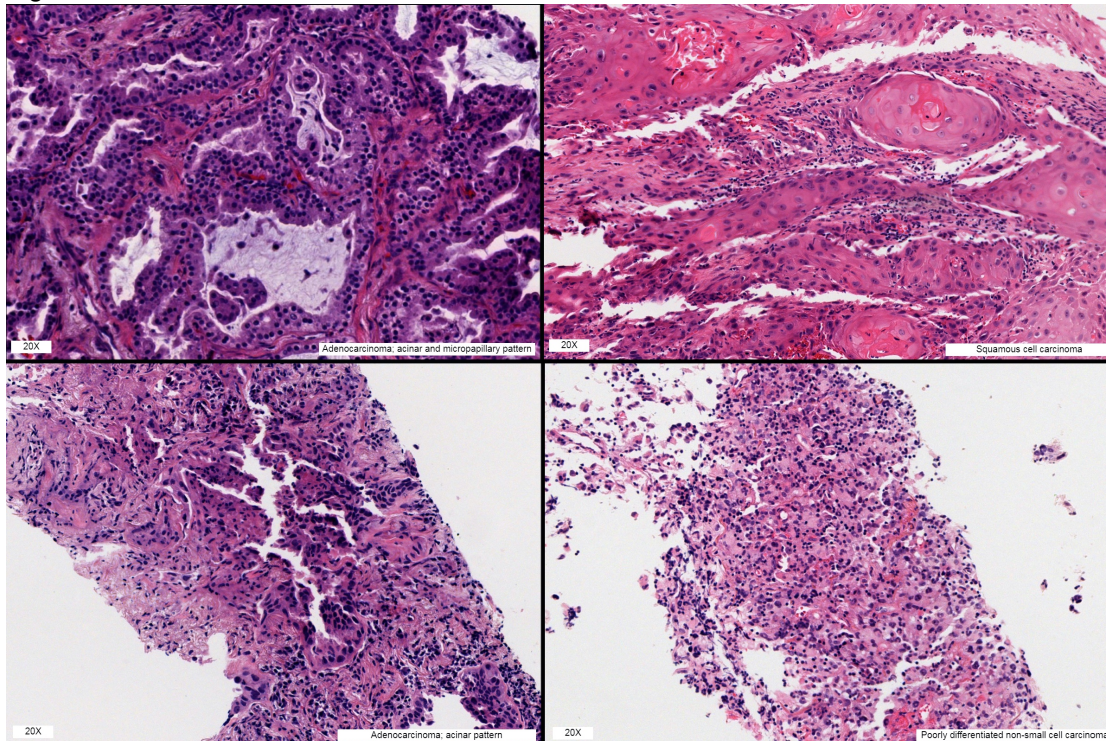
Figure 2 - 940

Case number	Age (years)	Sex	Ethnicity	Smoker	Histologic Type	Pattern/ Differentiation	Tumor Staging	PDL1 (22C3) expression by IHC	Chemo- therapy	Radio- therapy	Surgical Resection	Targeted therapy	Survival status	Overall Survival (months)
1	80	M	Caucasian	Yes	Adenocarcinoma	solid	IIIB	90	None	No	No	Not given	Alive	0
2	90	M	Caucasian	Yes	Adenocarcinoma	acinar, lepidic, micropapillary	II	0	None	No	No	Not given	Deceased	10
3	82	F	Caucasian	Yes	Adenocarcinoma	acinar	II	0	Carboplatin + Taxol	Yes	No	Capmatinib	Alive	15
4	74	F	African American	Yes	Adenocarcinoma	acinar	IV	<1	Carboplatin + Pemetrexed	No	No	Pembrolizumab	Alive	5
5	64	F	Caucasian	Yes	Adenocarcinoma	solid	IV	90	None	Yes	No	Pembrolizumab	Alive	7
6	71	M	Asian	NA	Adenocarcinoma	acinar	IVB	NA	NA	NA	NA	NA	NA	NA
7	70	F	African American	No	Squamous cell carcinoma	moderately differentiated	IIIB	90	Paclitaxol + Carboplatin	Yes	No	Durvalumab	Deceased	6
8	100	F	Caucasian	No	Adenocarcinoma	acinar, lepidic, micropapillary	IB	NA	None	Yes	No	Not given	Deceased	14
9	58	F	Caucasian	No	Poorly differentiated with squamous differentiation		IV	95	None	No	No	Crizotinib	Alive	16
10	76	F	Caucasian	Yes	Non-small cell carcinoma	poorly differentiated	IV	NA	Carboplatin + Alimta	Yes	No	Pembrolizumab	Deceased	18
11	90	F	Caucasian	No	Adenocarcinoma	poorly differentiated	IVA	30	None	No	No	Crizotinib	Deceased	17

Conclusions: In our cohort, *MET*ex14 skipping alterations were predominantly observed in adenocarcinomas in older age group. We also identified a novel 3 base pair deletion in intron 13 at -16 leading to *MET*ex 14 skipping. Due to diverse genomic mutations leading to *MET*ex14 skipping, some of the alterations may not be identified using DNA based sequencing alone due to incomplete coverage of the intronic regions, leading to false negative results. We recommend the use of RNA sequencing panels in NSCLC for *MET*ex14 detection.

941   Examination of PD-L1 and MHC Class I Expression in Non-Small Cell Lung Cancer Patients Receiving Immune Checkpoint Inhibitor Therapy

Margaret Moore[1], Anne Mills[1], Melson John[1], Richard Hall[2], Ryan Gentzler[1], Edward Stelow[2]
[1]University of Virginia, Charlottesville, VA, [2]University of Virginia Health System, Charlottesville, VA

Disclosures: Margaret Moore: None; Anne Mills: None; Melson John: None; Richard Hall: None; Ryan Gentzler: *Consultant*, AstraZeneca; *Consultant*, Pfizer; *Consultant*, BluePrint Medicines; *Grant or Research Support*, Pfizer, Merck, Bristol Myers-Squibb, Helsinn, Takeda, Jounce; Edward Stelow: None

Background: Major histocompatibility complex (MHC) class I functions in presentation of peptide antigens. In the tumor immune environment, MHC class I enables activation of cytotoxic T-cells, and loss of expression is a proposed mechanism of failure of immune checkpoint inhibitor (ICI) therapy. We hereby examine the expression of PD-L1 and MHC class I in patients with non-small cell lung cancer (NSCLC) who received anti-PD-1/PD-L1 ICI therapy.

Design: The institutional lung cancer registry was queried to identify patients with stage IV or recurrent NSCLC diagnosed between 2008 and 2018. Clinical and radiologic data were abstracted from the medical record. Patients who received at least 2 consecutive doses of an anti-PD-1/PD-L1 ICI (pembrolizumab, atezolizumab, nivolumab) were selected. Immunohistochemistry (IHC) for PD-L1 (SP142) and MHC class I (Abcam, EMR8-5) was performed on diagnostic FFPE tissue for each case. Tumor cell PD-L1 staining was scored as negative (<1%), low-positive (1-50%), or high-positive (>50%). MHC class I staining was classified as intact, partial loss, or complete loss.

Results: 60 cases were identified: 34 adenocarcinomas, 20 squamous cell carcinomas, 1 adenosquamous carcinoma, and 5 NSCLC not otherwise specified. 44 patients received an ICI in isolation; 16 received an ICI in combination with chemotherapy. 42 cases (70%) demonstrated intact MHC class I expression; 4 (7%)

demonstrated partial loss; and 14 (23%) showed complete loss. There was no significant correlation between MHC class I expression and radiologic response on initial surveillance scan. PD-L1+/MHC- cases demonstrated the longest median progression-free survival (PFS,18.4 mos), but this did not reach statistical significance when compared to PFS of patients that were PD-L1+/MHC+ (5.6 months), PD-L1-/MHC+ (9.0 mos), and PD-L1-/MHC- (6.4 mos, p=0.137). 7 patients with MHC class I loss had durable response to ICI therapy, with PFS greater than 12 months. There was a non-significant trend of longer PFS in patients with high-positive PD-L1 expression (21.7 mos) when compared to PD-L1 negative and low-positive patients (6.4 mos, p=0.114).
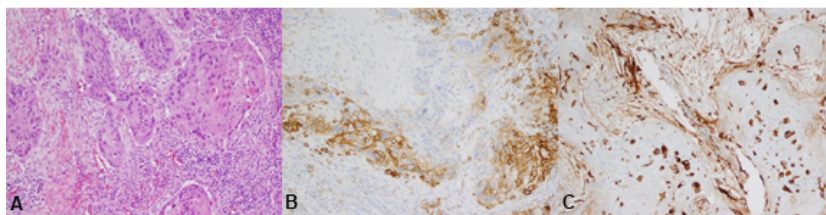
Figure 1 - 941

Figure 1. PD-L1 and MHC class I expression in patient with durable response to nivolumab. (A) H&E demonstrates a poorly differentiated squamous cell carcinoma accompanied by a robust lymphocytic inflammatory infiltrate. (B) IHC for PD-L1 demonstrates membranous staining in a subset of the tumor cells (~30% of total sampled tumor) and in occasional infiltrating immune cells. (C) IHC for MHC class I demonstrates complete loss of staining in the tumor cells, with retained expression in the infiltrating immune cells and stromal elements.

Figure 2 - 941
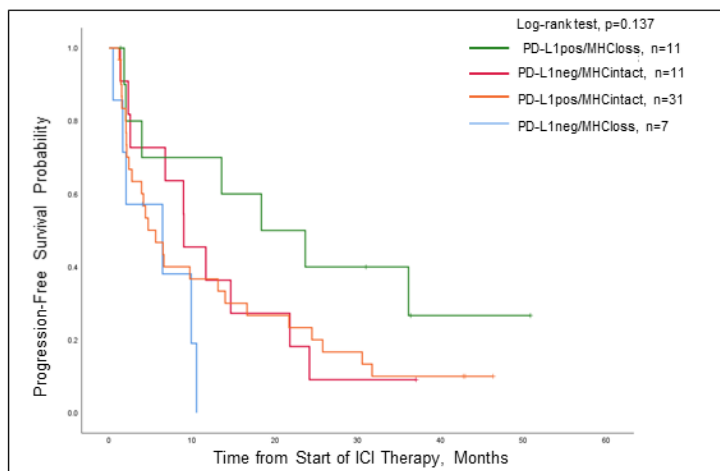
Figure 2. Progression-free survival by PD-L1 and MHC class I expression.

Conclusions: In this small pilot study of NSCLC patients, dual IHC interpretation for PD-L1 and MHC class I was not reliably predictive of radiologic response or PFS after initiation of ICI therapy. Multiple patients with MHC class I loss demonstrated prolonged treatment response. Examination of these markers in an expanded case series is warranted.

942   Diagnosis Migration with the New 2020 Hypersensitivity Pneumonitis Guideline
Mutsumi Ozasa[1], Wataru Uegami[2], Andrey Bychkov[3], Junya Fukuoka[4]
[1]Nagasaki University Graduate School of Biomedical Sciences, Nagasaki, Japan, [2]Kamogawa, Japan, [3]Kameda Medical Center, Kamogawa, Japan, [4]Nagasaki University, Nagasaki-shi, Japan

Disclosures: Mutsumi Ozasa: None; Andrey Bychkov: None; Junya Fukuoka: None

Background: Hypersensitivity pneumonitis (HP) has several overlapping characteristics with interstitial pneumonia (IP), which creates a high rate of discordance in diagnosing HP. Until recently, there have been no consensus criteria for pathological diagnosis of HP, and most pathologists make diagnosis of HP based on the local experience. The 2020 clinical practice guidelines, highly influenced by pathology, were developed to standardize HP diagnosis and to avoid misdiagnosis with other IP entities. The aim of our study was to evaluate the effect of the 2020 HP guidelines on cases diagnosed as IP.

Design: Cases with fibrotic IP diagnosed in 2014–2019 were classified according to the 2020 HP guidelines into three categories: typical HP, probable HP, and indeterminate HP. The original pathological diagnosis and categorization based on the HP guidelines were compared. The clinical data including serum data and pulmonary function test were compared among groups.

Results: A total of 271 consecutive IP cases with available lung biopsy were enrolled and 63 of them were excluded because of the presence of strong histological autoimmune features such as plasma cell infiltration or extensive lymphoid follicles. Eventually, 208 cases were classified into typical HP (n = 30), probable HP (n = 63), and indeterminate for HP (n = 115) using the 2020 HP guidelines. Number of cases changed from original diagnosis of not HP to HP diagnosis by the 2020 guidelines were 65 (24%). The clinical data of those cases were more identical to the cases diagnosed as indeterminate for HP than typical or probable HP. None of the cases with original HP diagnosis was diagnosed as indeterminate for HP by the 2020 HP guidelines.

Conclusions: We confirmed that pathological criteria of the 2020 HP guideline efficiently exclude not HP cases. At the same time, approximately one-fourth of all cases of fibrotic IP meet diagnostic change from not HP to fibrotic HP, which may not correlate with clinical features of HP.

---

943   PAX1 Shows Variable Expression in Thymic Epithelial Neoplasms and Morphologic Mimics

Paige Parrack[1], Jason Hornick[2], Lynette Sholl[1]
[1]Brigham and Women's Hospital, Boston, MA, [2]Brigham and Women's Hospital, Harvard Medical School, Boston, MA

Disclosures: Paige Parrack: None; Jason Hornick: None; Lynette Sholl: *Grant or Research Support*, Genentech

Background: Thymic epithelial neoplasms are morphologically diverse and can pose diagnostic challenges, particularly in biopsy specimens. Immunohistochemistry (IHC) using a polyclonal PAX8 antibody is commonly used to highlight the thymic epithelial component, but this marker is not completely sensitive and specific for thymic neoplasms. The PAX1 transcription factor plays an important role in thymus development, and in murine models, PAX1 was found to be retained in a subset of adult thymic epithelial cells. The goal of this study was to determine if PAX1 IHC would be useful in the distinction between primary thymic epithelial neoplasms and histologic mimics.

Design: A search of the departmental pathology records was conducted for primary thymic neoplasms, sarcomatoid mesotheliomas, and squamous cell carcinomas (SCCs). PAX1 IHC using a rat monoclonal antibody (Millipore, clone 5A2) was performed on whole tissue sections from biopsy and resection specimens of 36 thymomas, 9 thymic carcinomas, 8 thymic neuroendocrine tumors (NETs), 15 head and neck SCCs, 13 lung SCCs, 10 sarcomatoid mesotheliomas, 5 anal SCCs, 4 esophageal SCCs, and 1 sarcomatoid carcinoma. Two pathologists evaluated the percentage of tumor cells with nuclear staining (0-100%) and the intensity of staining (0-3) and quantified the results with an H score (0-300). Tumors with <1% weak (1) staining were considered negative.

Results: Variable PAX1 staining was present in 100% of thymomas (mean/range H-score: 146/10-270), 89% of thymic carcinomas (mean/range H score: 89/0-240), and 87% of thymic NETs (mean/range H score: 87/0-200).   Lower PAX1 expression was identified in 31% of non-thymic neoplasms (mean/range H score: 5/0-70), including 7 head and neck SCCs, 6 lung SCCs, 1 mesothelioma, and 1 anal SCC. Multiple resection specimens showed geographic reduction in staining consistent with compromised antigenicity from suboptimal fixation.   The scoring cutoff optimized for sensitivity for thymic neoplasms (all H-values) leads to a specificity of 68.8%; optimized for specificity (H values greater than or equal to 75) leads to a drop in sensitivity to 73.6%.

Conclusions: Overall, PAX1 expression by IHC has a high sensitivity for thymic epithelial neoplasms and stronger staining in the thymic tumors compared to mesotheliomas and SCCs. However, the wide staining variability in thymic epithelial neoplasms and sensitivity of the antibody to fixation effects may lead to difficulty with interpretation, suggesting that this marker is unlikely to supplant polyclonal PAX8 in diagnostic practice.

---

944 Factors Influencing the Tumor Spread through Airway Space (STAS) Identification during Intraoperative Consultation

Raghavendra Pillappa[1], Valentina Robila[2], Jonathan Edwards[3]
[1]VCU Health System, Richmond, VA, [2]Virginia Commonwealth University Health System, Richmond, VA, [3]Richmond, VA

Disclosures: Raghavendra Pillappa: None; Valentina Robila: None; Jonathan Edwards: None

Background: Identification of STAS is considered a significant risk factor for increased local recurrence in patients treated with limited resection for lung cancer. The utility of frozen section evaluation for the presence of STAS is debated due to insufficient data. Recent studies have described that the presence of ample non-neoplastic alveolated parenchyma is required to adequately assess STAS in frozen section slides. Our study investigates the requirements for STAS identification on frozen sections, including the extent of STAS clusters and the adequacy of tumor adjacent non-neoplastic parenchyma.

Design: Frozen sections slides of lung adenocarcinoma surgical resections were retrospectively reviewed by two pathologists, to assess the presence of STAS meeting the WHO criteria, and tabulate the presence of low STAS (1-4 clusters), intermediate STAS (5-10 clusters), and high STAS (>10 clusters) and the availability of the non-neoplastic parenchyma (NNP) in frozen and permanent slides, respectively.

Results: A total of 166 lung adenocarcinoma cases with surgical resection and intraoperative consultation between 2015-2016 were retrospectively reviewed. Frozen sections slides of 142 (85.5%) cases contained predominantly tumor, without adjacent non-neoplastic parenchyma (NNP) for STAS assessment were excluded. Of the remaining 24 cases, low and intermediate STAS was identified on 9 (37.5%) frozen sections, all confirmed on permanent controls and additional tumor sections (Table 1, Figures 1A/1B, high STAS; 2A/2B, low STAS). In 5 (20.8%) cases, the tumor associated STAS was not present on frozen slides. This was due to lower STAS burden and more limited NNP, measuring 1mm to 5 mm on frozen compared to 2mm to 8 mm on permanent, sections. The sensitivity and negative predictive values were moderate at 64% and 67% respectively, while both specificity and positive predictive values were 100% each. Peritumoral fibrosis/ inflammation and artifacts such as linear stripping and tissue fragmentation are prevalent challenges on frozen tissue. Only one case positive for STAS on the intraoperative consultation had a completion lobectomy, and 2 (14.2%) cases had local recurrence at 2 and 4 years respectively.

STAS (clusters numbers)	STAS Present (Both)		STAS (Discrepant cases)	
	Frozen Slides (NNP, mm)	Permanent Slides (NNP, mm)	Frozen slides (NNP, mm)	Permanent slides (NNP, mm)
Low (1-4)	3 (1.0-5.0)	1 (12.0)	0 (1.0-2.0)	3 (2.0 to 8.0)
Intermediate (5-10)	6 (3.0-8.0)	2 (5.0)	0 (2.0-5.0)	2 (3.0-8.0)
High (>10)	-	6 (9.0-14.0)	-	

Figure 1 - 944
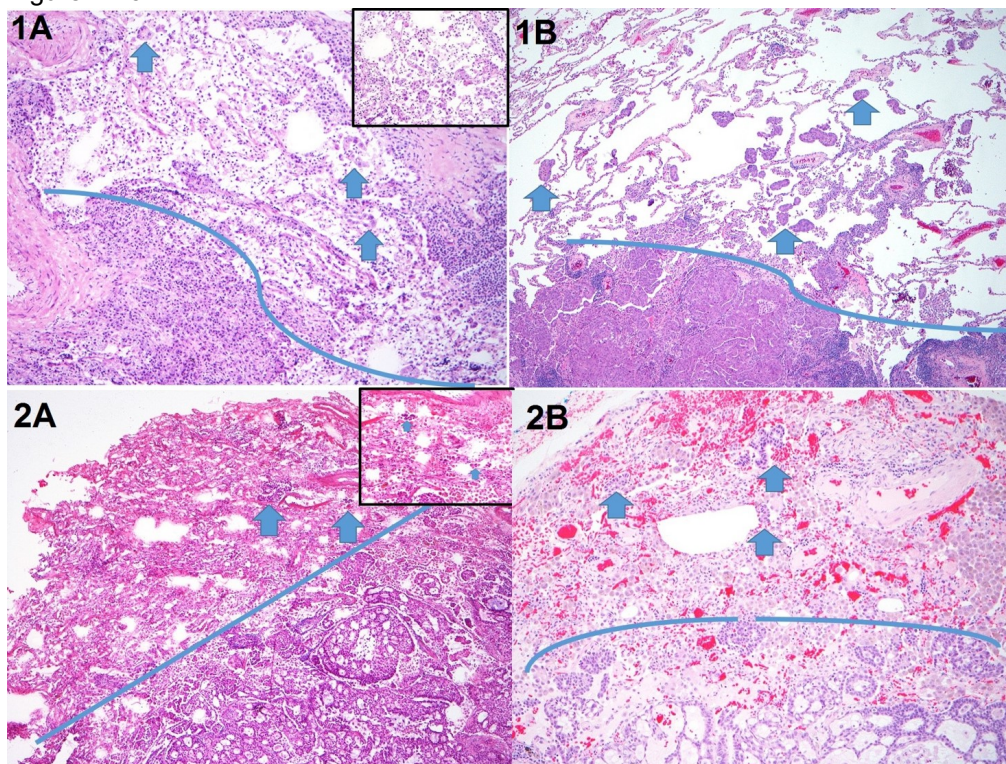
Conclusions: Despite artifactual challenges, identification of STAS on frozen sections has high specificity and positive predictive value. The number of STAS clusters identified on intraoperative consultation is increased in high STAS tumors and when more non-neoplastic parenchyma is evaluated. Given its clinical impact, the value of the frozen section for STAS detection needs standardization of tissue evaluation for best operative management.

945   Spread Through Air Spaces (STAS) in Stage 1 Lung Adenocarcinoma: Comparison of Its Prevalence and Prognostic Significance between Two Academic Institutions

Treah May Sayo[1], Julian Villalba[2], Keiko Kunitoki[2], Fang Zhou[3], Angela Shih[4], Yin Hung[4], Andre Moreira[5], Mari Mino-Kenudson[2]
[1]Massachusetts General Hospital, Lung Center of the Philippines, Boston, MA, [2]Massachusetts General Hospital, Harvard Medical School, Boston, MA, [3]NYU School of Medicine, New York, NY, [4]Massachusetts General Hospital, Boston, MA, [5]NYU Langone Health, New York, NY

Disclosures: Treah May Sayo: None; Julian Villalba: None; Keiko Kunitoki: None; Fang Zhou: None; Angela Shih: None; Yin Hung: None; Andre Moreira: None; Mari Mino-Kenudson: *Consultant*, H3 Biomedicine; *Consultant*, AstraZeneca; *Grant or Research Support*, Novartis

Background: Growing evidence suggests the prognostic significance of SATS in patients with early-stage lung adenocarcinoma, in particular, those with sublobar resection. However, published studies used various definitions for STAS; the diagnosis of STAS may be subject to interobserver variability that, in turn, may result in the difference in prevalence and prognostic significance of STAS across institutions.

Design: The study cohort consisted of stage 1 lung adenocarcinomas resected at two institutions (cohort A: n=283; cohort B: n=198) during similar time periods with similarly decent follow-up. Both institutions had applied similar grossing/processing protocols. The prevalence of STAS and its association with clinicopathologic variables, recurrence free survival (RFS), and overall survival (OS) were compared between the cohorts. The variables included type of operation, AJCC 8th stage, histologic grade, as well as the presence of lepidic, micropapillary (mPAP), or solid (SOL) patterns (5% cut-off for presence).

Results: The prevalence of STAS was 7% in cohort A and 39% in cohort B (p<0.0001). The tumor histologic grade (high grade: 21% in A vs. 37% in B, p=0.0001) and AJCC stage (Stage 1B: 19% in A vs. 13% in B, p=0.048) also differed between the cohorts, while no difference was seen in the other variables. STAS was associated with high grade histology, the absence of lepidic and the presence of mPAP and SOL patterns (p<0.01 for all) in both cohorts, while it was also associated with stage 1B in cohort A (p=0.016). In multivariate analysis, STAS was associated with high grade histology (p<0.0001) and marginally with the presence of mPAP (p=0.065) in cohort A, and lobectomy (p=0.016), the presence of mPAP (p<0.0001) and SOL (p=0.027) in cohort B. Regarding survival, STAS was associated with shorter RFS (p=0.030) and OS (p=0.048) in cohort B and with shorter OS (p=0.040) and marginally with shorter RFS (p=0.060) in the sublobar resection subset of cohort B by univariate analysis, while STAS had no bearing on survival in the lobectomy subset or cohort A. Of note, no difference in RFS and OS was seen as a whole between the cohorts.

Conclusions: The prevalence and prognostic significance of STAS differ between the two institutional cohorts. While this may be explained in part by the difference in patient populations, subjectivity to the diagnosis of STAS may potentially contribute. Additional multi-institutional studies to better define and improve reproducibility of STAS are warranted.

946   **Somatic Mutation of BAP1 Can Lead to Expression Loss in Non-Small Cell Lung Carcinoma: Next Generation Sequencing and IHC Analysis in A Large Single Institute Cohort**

Tong Sun[1], Christine Minerowicz[2], Harold Sanchez[3], William Laskin[4], Paul Cohen[5], Minghao Zhong[4]
[1]Yale New Haven Hospital, Yale School of Medicine, New Haven, CT, [2]Yale New Haven Healthcare, New Haven, CT, [3]Yale New Haven Health Bridgeport, New Haven, CT, [4]Yale School of Medicine, New Haven, CT, [5]Yale University School of Medicine, New Haven, CT

Disclosures: Tong Sun: None; Christine Minerowicz: None; Harold Sanchez: None; William Laskin: None; Paul Cohen: None; Minghao Zhong: None

Background: As a tumor suppressor, germline and somatic inactivation of BRCA1 associated protein 1 gene (BAP1) with loss of expression is a relatively common finding in mesothelioma, melanocytic tumors, clear cell renal cell carcinoma and several other epithelial, mesenchymal and neural tumors. Incidence of BAP1 genetic alterations and subsequent expression loss has not been well established in non-small cell lung carcinoma (NSCLC) by large-scale studies.

Design: With IRB approval, a total of 356 NSCLC cases received between July 2016 and June 2020 in our institute were reviewed for the current study. All cases underwent a comprehensive target cancer gene next generation sequencing test (Oncomine Assay) with tumor and paired germline control specimen (peripheral blood or buccal mucosa). The majority of the cases (259, 73%) were from primary lung tumor, while 97 cases (27%) were from lymph node or distant organ metastases. Among them, 214 (60%) were adenocarcinoma, 89 (25%) were squamous cell carcinoma, and 53 (15%) were diagnosed as "non-small cell lung carcinoma" without specified subtype. After BAP1 genetic alteration was confirmed, the protein expression status of *BAP1* was subsequently evaluated by immunohistochemistry (IHC).

Results: BAP1 somatic missense mutations were detected in 6 NSCLC cases (incidence: 1.7%). Clinical, pathological and molecular characteristics of these 6 cases, including other detected genetic alterations, are summarized in Table 1. Briefly, cases harboring BAP1 mutations were diagnosed with more aggressive pathologic features, and all carried at least one additional genetic alteration, suggesting BAP1 mutation is a later "passenger" alteration in NSCLC carcinogenesis. In subsequent IHC study, one adenocarcinoma which harbored two different missense BAP1 mutations, and another which carried bioinformatically predicted deleterious BAP1 mutation, showed complete protein expression loss (Figure 1, Case #4 and Case #5).

Table 1. Clinical, pathological and molecular characteristics of lung non-small cell carcinoma with BAP1 mutation

Case #	Age/ Gender	Tested Specimen	Pathology diagnosis	Genetic Alterations of EGFR/ROS1/ALK/KRAS/RET/BRAF	Other Genetic Alterations	Somatic Mutation in BAP1	Expression of BAP1 Protein by IHC
1	49/F	Lung primary	Adenocarcinoma	KIF5B-RET gene fusion	TSC1 p.G193R SETD2 p.G2091Ter	p.G41S	Retained
2	80/F	Adrenal metastasis	Adenocarcinoma with mucinous features	KRAS p.G12A	N/A	p.C39F	Retained
3	67/M	Lung primary	Poorly differentiated squamous cell carcinoma	N/A	TP53 p.Y220H NOTCH1 p.Q1837Ter TSC1 p.P362S	p.T16I	Retained
4	50/F	Lung primary	Adenocarcinoma	KIF5B-RET gene fusion	N/A	p.L86Q; p.V99E	Loss
5	63/F	Lymph node metastasis	Poorly differentiated adenocarcinoma	N/A	TP53 p.R156P NF1 p.S144 Ter PDGFRA p.M578K NF1 R1476H	p.L18F	Loss
6	78/M	Liver metastasis	Poorly differentiated squamous cell carcinoma	N/A	PTEN p.G44S TP53 p.I255F CDKN2A p.Y44Ter FBXW7 p.E115_del POLE p.V1613fs	p.E125Q	Retained

Figure 1 - 946
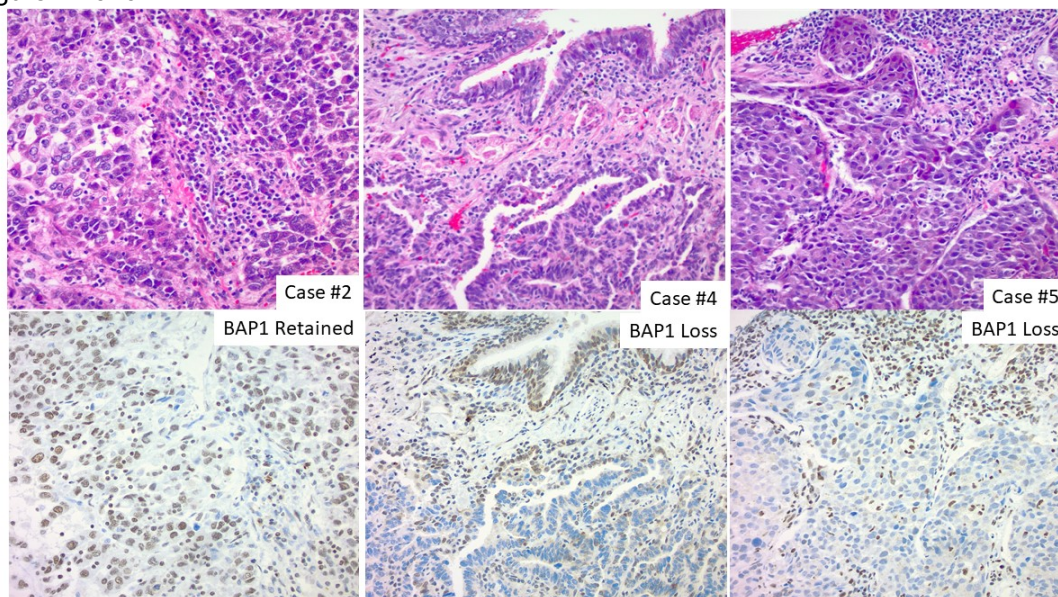
Figure 1 . Representative lung adenocarcinoma cases with immunohistochemical stain of BRCA1-associated protein 1 (BAP1, lower panel) and corresponding H&E sections (upper panel).

Conclusions: Compare with other known *BAP1* loss associated malignancy such as mesothelioma, inactivation of BAP1 by somatic mutation is a very rare occurrence in NSCLC. BAP1 mutations and expression loss in NSCLC is associated with more advanced disease and accompanied with other complex genetic alternations.

947   Atypical Thymomas with Squamoid and Spindle Cell Features: Clinicopathologic, Immunohistochemical and Molecular Genetic Study of 120 Cases with Long-Term Follow-up

David Suster[1], Marcello Distasio[2], Alexander Mackinnon[3], German Pihan[4], Saul Suster[5]
[1]Rutgers New Jersey Medical School/Rutgers University, Newark, NJ, [2]Yale School of Medicine, Yale New Haven Hospital, New Haven, CT, [3]The University of Alabama at Birmingham, Birmingham, AL, [4]Beth Israel Deaconess Medical Center, Boston, MA, [5]Medical College of Wisconsin, Milwaukee, WI

Disclosures: David Suster: None; Alexander Mackinnon: None; German Pihan: None

Background: Thymomas represent the most common type of primary thymic epithelial neoplasm. Due to their variegated morphologic appearance, the histopathologic classification of thymoma may be difficult, particularly the distinction between WHO types B3 and B2 or thymic carcinoma.

Design: 120 atypical thymoma (WHO B3) resections were collected and assessed for age, sex, clinical symptoms, size of the tumor, extent of resection, margin status, clinical staging, histopathologic features and clinical follow up. A total of 92 cases (42 by tissue microarray, 50 by whole slide section) were tested with an antibody panel of p40, p63, cytokeratin AE1/AE3, PAX8, EMA, chromogranin, synaptophysin, calretinin, CD3, TdT, bcl-2, CD20, CD5, CD117 and MIB1. Next generation sequencing using a 50 gene panel was performed on a subset of 50 samples. Predictive pathologic features were evaluated with respect to recurrence, overall survival, and metastasis by construction of Kaplan-Meier plots and multivariate analysis logistic regression.

Results: The patients were 63 men and 57 women who presented with a discrete anterior mediastinal mass measuring from 2 to 23 cm (mean: 8.2 cm). Patient age ranged from 14 to 86 years (mean: 57.8) and most presented with symptoms referable to a mass lesion. 18 patients had concomitant myasthenia gravis or other autoimmune disorders. 79 cases were characterized by predominantly round to polygonal tumor cells showing sheet-like growth; 29 cases showed sheets of oval or spindle cells. 12 cases showed a combination. Thymic carcinoma arose from a B3 thymoma in 16 cases. A lymphoid cell component was present at least focally in most cases with positivity for CD3, TdT, bcl-2 and CD20 (focal). 92 cases (100%) were positive for p40, p63 and cytokeratin. 21 cases (23%) were positive for CD5 and 12 (13%) for CD117. MIB1 proliferation index was increased (mean= 11.6%) compared to non-B3 thymoma. EMA and PAX8 showed scattered positivity. Other IHC markers were nearly uniformly negative. Next generation sequencing analysis did not disclose any clinically significant variants. Clinical follow up ranging from 2-29 years showed a progressively aggressive behavior and fatality rate with advancing stage. Statistical analysis showed that incompletely resected tumors and tumors diagnosed at an advanced clinical stage (III or IV) showed worse overall and recurrence free survival.

Figure 1 - 947
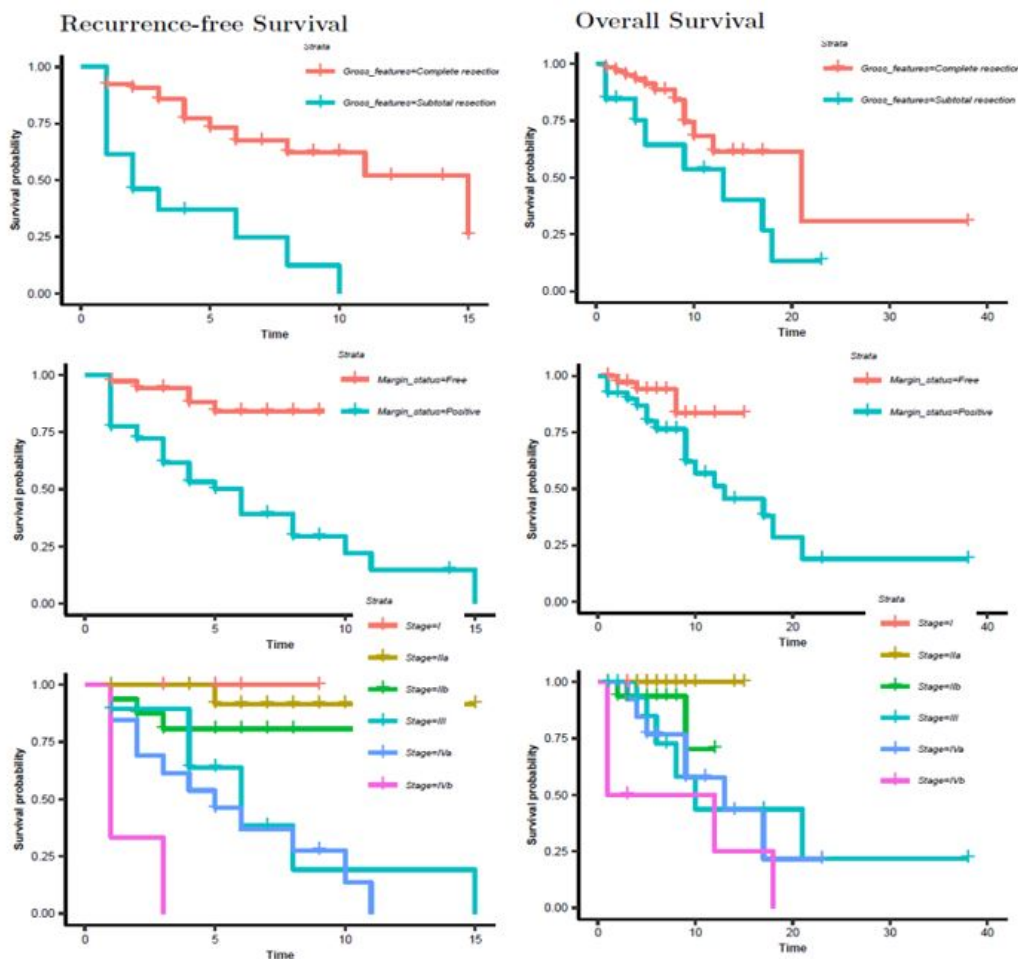
Kaplan-Meier survival curve estimates were constructed for recurrence-free (left column) and overall (right column) survival, highlighting the effects of complete resection and margin status on clinical outcomes, as well as an increase in aggressive behavior with increasing clinical stage at time of resection. These features were all found to be statistically significant predictors of outcome (p << 0.05) on log-rank tests for both recurrence-free and overall survival.

Conclusions: Atypical (WHO B3) thymomas show increased cytologic atypia, higher proliferation index compared to non-B3 thymomas, and a protracted and slowly progressive clinical course with a potential for transformation to higher grade malignancy and fatal outcome in some cases. A small percentage of atypical thymomas will show positive staining for CD5 and CD117. Completeness of resection and stage at time of diagnosis appear to be the most clinically significant variables with regards to overall survival.

948 Immunohistochemical Evaluation of SMARCA4 and SMARCA2 Expression in Tumors from Various Organs

Stephen Wall[1], Jianhui Shi[1], Angela Bitting[1], Haiyan Liu[1], Fan Lin[1]
[1]Geisinger Medical Center, Danville, PA

Disclosures: Stephen Wall: None; Jianhui Shi: None; Angela Bitting: None; Haiyan Liu: None; Fan Lin: None

Background: SMARCA4-deficient thoracic sarcoma (SMARCA4-DTS) is a recently described entity with an aggressive clinical course, defined as a poorly differentiated tumor with rhabdoid morphology, co-loss of SMARCA4 and SMARCA2, and overexpression of SOX2 (Perret P et al. AM J Surg Pathol 2019;43:455-465). The expression

of these 2 markers has not been extensively studied nor reported in the literature. In this study, we investigated the loss of SMARCA2 and/or SMARCA4 expression in a large series of tumors from various organs.

Design: Using the Leica Bond III staining platform, immunohistochemical (IHC) detection of SMARCA4 (EPNCIR111A; 1:200; Abcam) and SMARCA2 (D9E8B; 1:100; Abcam) expression was performed on tissue microarray sections containing 1,638 tumors, including 20 bladder small cell carcinomas (CA), 43 urothelial CA, 81 breast ductal CA, 30 chromophobe renal cell carcinomas (RCC) and oncocytomas, 122 low-grade and high-grade clear cell RCC, 126 colonic adenocarcinomas (ADC), 25 endocervical ADC, 97 endometrioid ADC, 49 squamous cell carcinomas (SCC) of head/neck, 78 esophageal ADC, 50 hepatocellular carcinomas, 11 intrahepatic cholangiocarcinomas, 228 lung ADC, 139 lung SCC, 61 lung neuroendocrine carcinomas, 16 mesotheliomas, 50 pancreatic ADC, 32 pancreatic neuroendocrine tumors, 36 prostatic ADC, 47 renal urothelial CA, 85 seminomas, 33 melanomas, 28 Merkel cell CA, 52 testicular tumors, 51 follicular adenoma, and 48 papillary thyroid CA. The staining results were recorded as positive when complete loss of either SMARCA2 or SMARCA4 expression with strong internal positive control was seen. All positive cases were further confirmed by repeating IHC for either SMARCA4 or SMARCA2 on the matching routine tissue sections. IHC for SOX2 was also performed on these positive cases.

Results: The cases with loss of expression of either SMARCA4 or SMARCA2 are summarized in Table 1. Co-loss of SMARCA4 and SMARCA2 was not identified. Loss of SMARCA4 was only seen in 4 lung ADCs and 1 urothelial CA. In contrast, loss of SMARCA2 was present in a wider range of tumor types. None of the SMARCA4 or SMARCA2 loss cases showed rhabdoid morphology. All cases with either SMARCA4 or SMARCA2 loss were negative for SOX2. All other tumors mentioned above showed intact expression of both markers. Representative cases are showed in Figures A and B.

Table 1. Summary of Cases with Loss of Expression of SMARCA4 or SMARCA2

Diagnosis	Loss of SMARCA2	Loss of SMARCA4
Bladder urothelial CA (N=43)	0	1
Colon ADC (N=126)	1	0
Endometrial CA (N=97)	10	0
Esophageal ADC (N=78)	4	0
Hepatocellular CA (N=50)	1	0
Lung ADC (N=228)	7	4
Lung SCC (N=139)	3	0
Mesothelioma (N=16)	1	0
Testicular Tumors (N= 52)	4	0

Figure 1 - 948
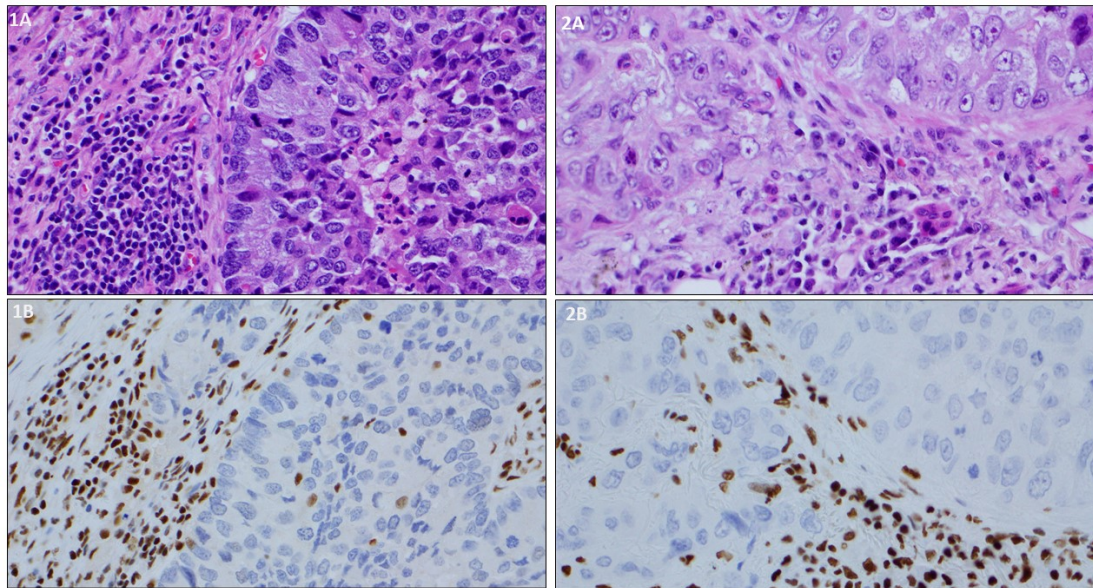
Case of pulmonary adenocarcinoma, H&E (1A) and IHC showing loss of SMARCA2 (1B)

Additional case of pulmonary adenocarcinoma, H&E (2A) and IHC showing loss of SMARCA4 (2B)

Conclusions: Our data support the findings in the above publication, that co-loss of SMARCA4 and SMARCA2 is highly specific for diagnosing SMARCA4-DTS. SOX2 expression is not seen in the cases with loss of expression of either SMARCA4 or SMARCA2; therefore, SOX2 can be used as a screening marker to identify SMARCA4-DTS in a small biopsy or cytologic sample. Further study to investigate the clinical significance of the subset of carcinomas with loss of either SMARCA4 or SMARCA2 in this study is warranted.

949 Comprehensive Profiling of Lung Adenosquamous Carcinoma Demonstrates High Frequency of Targetable Genomic Alterations
Sarah Wu[1], Jacob Sands[2], Lynette Sholl[1]
[1]Brigham and Women's Hospital, Boston, MA, [2]Dana-Farber Cancer Institute, Boston, MA

Disclosures: Sarah Wu: None; Jacob Sands: *Advisory Board Member*, AstraZeneca; *Consultant*, AstraZeneca; *Advisory Board Member*, Medtronic; *Advisory Board Member*, Jazz Pharmaceuticals; Lynette Sholl: *Grant or Research Support*, Genentech

Background: Adenosquamous carcinoma of the lung is associated with an aggressive disease course and poor prognosis. It is a rare subtype of non-small cell lung carcinoma that is underrepresented in comprehensive tumor genetics studies such as The Cancer Genome Atlas and remains poorly characterized. Prior studies using focused gene panels have identified EGFR and KRAS mutations, highlighting a deficiency of genomic scope of analysis in the characterization of this lung cancer subtype. Uncertainty regarding the value of biomarker testing among patients with this diagnosis may hamper access to effective targeted therapies.

Design: We performed a retrospective analysis of institutional cases received between 2015 and 2020 to identify 36 lung adenosquamous carcinoma diagnoses, based on the WHO criteria, that underwent prospective next generation sequencing of exonic DNA for 447 cancer genes. We performed a chart review to identify patient characteristics including age, gender, and smoking status.

Results: Of the 36 cases of lung adenosquamous carcinoma, female patients comprised 64%. At the time of diagnosis, 20.0% were stage 1, 14.3% were stage 2, 28.6% were stage 3, and 37.1% were stage 4. 44% were biopsies and 56% were resections. Smoking histories were available for 31 patients, with an average number of 24 pack years. To delineate trends based on smoking status, we assigned patients into categories of non-smokers (8/31, 25.8%), light smokers (less than or equal to 10 pack years, 6/31, 19.4%), and heavy smokers (greater than 10 pack years, 17/31, 54.8%). The average age of all patients was 69 years old, with an average age of 62 for non-

smokers, 71 for light smokers, and 69 for heavy smokers. The most common driver alterations overall occurred in EGFR (8) followed by MET (8) and KRAS (6). By sorting the patients by smoking status, we identified a targetable alteration in all 14 non-smoker and light smoker patients, including EGFR (7), MET (6), and ERBB2 mutations (1). 24% of heavy smokers had targetable alterations, including KRAS G12C (2), EGFR (1) and MET (1) mutations. TP53 mutation was the most common alteration overall (15/36, 41.6%), enriched in heavy smokers (59%). STK11 alterations were detected in 5/17 (29%) of heavy smokers.

Conclusions: In this large cohort of patients with lung adenosquamous carcinoma, all never and light smokers and over 20% of heavy smokers had a driver alteration predictive of response to targeted therapies. This data highlights the essential role of comprehensive biomarker testing for all advanced stage patients with lung adenosquamous carcinoma to improve patient outcomes.

950   Not a General Neuroendocrine Marker, Islet-1 Is Selectively Expressed in Small Cell Carcinoma and Thymoma

Yan Xiang[1], Nicole Hackman[1], Amy Ziober[1], Paul Zhang[1]
[1]Hospital of the University of Pennsylvania, Philadelphia, PA

Disclosures: Yan Xiang: None; Nicole Hackman: None; Amy Ziober: None; Paul Zhang: None

Background: Islet-1 (Isl1), a LIM-homeodomain transcription factor, plays key roles in programming the epigenome and facilitating recruitment of additional regulatory factors during successive cell lineage specification and differentiation steps. Despite the efforts of a few studies to test the specificity and sensitivity of Isl1 as a marker of pancreatic neuroendocrine tumors, detailed insights of Isl1 in other tumor types are critically missing.

Design: Ninety different types of solid tumors were examined. These include intraductal papillary mucinous neoplasm (IPMN, n=2) of the pancreas, lung adenocarcinoma (LAC, n=5), papillary thyroid carcinoma (PTC, n=5), parathyroid adenoma (PA, n=5), mesothelioma (Meso, n=8), adrenal cortical carcinoma (ACC, n=5), breast carcinoma (BC, n=5), squamous cell carcinoma (SCC, n=5), neuroendocrine tumor of pancreas (PNET, n=13) and intestine (INET, n=11), carcinoid tumor of lung (LCT, n=6), lung small cell carcinoma (LSCC, n=4), thymoma (TM, n=8), paraganglioma/pheochromocytoma (PG/Pheo, n=8). Immunohistochemistry studies using antibody (Clone EP283) directed against Isl1 were performed and the staining results were scored semi-quantitatively.

Results: Strong and diffuse Isl1 nuclear staining was observed in normal pancreatic islet, thymic epithelium and adrenal medulla. Similar expression was detected in PNET (100%), PG/Pheo (100%), TM (88%) and LSCC (75%). Isl1 was less frequently detected in meso(13%), ACC (20%), BC (20%), INET (27%), SCC (60%), usually in focal fashion. Isl1 was not detected in other NET such as LCT, PA and other non-NET such as IPMN, LAC, and PTC.

Conclusions: Isl1 was selectively expressed in different NET and non-NET. It's expression in Pheo/PG, PNET and TM likely represents a lineage marker for these tumors. However, it's expression in LSCC but not LCT is interesting that might further implicate a different origin of LSCC from LCT. In addition to a marker for certain NET such as PNET, PG/Pheo, Isl1 may also be useful for diagnosis of LSCC vs. LCT in small specimen, and diagnosis of TM against LAC and Meso in mediastinum. Little is known about the role of Isl1 in tumorogenesis, further investigation is warranted.

951   Microsatellite Instability and Mismatch Repair Deficiency in Smoking-Associated Lung Carcinoma

Soo-Ryum Yang[1], Jason Chang[1], Erika Gedvilaite[1], John Ziegler[1], Jennifer Sauter[1], Natasha Rekhtman[1], William Travis[1], Marc Ladanyi[1]
[1]Memorial Sloan Kettering Cancer Center, New York, NY

Disclosures: Soo-Ryum Yang: None; Jason Chang: None; Erika Gedvilaite: None; John Ziegler: None; Jennifer Sauter: None; Natasha Rekhtman: None; William Travis: None; Marc Ladanyi: None

Background: Microsatellite instability (MSI) and mismatch repair (MMR) deficiency represent a distinct model for carcinogenesis and predict response to immunotherapy. The clinicopathologic features of MSI and MMR deficiency in lung carcinomas have not been previously characterized.

Design: MSI status from 5,526 patients with lung cancer was analyzed from targeted next-generation sequencing (NGS) data using validated bioinformatic pipelines. Select cases were evaluated using a PCR-based MSI assay (Idylla) and/or MMR immunohistochemistry (IHC). Cases were classified as MSI-high (MSI-H) if confirmed by at least two methods.

Results: In all, 27/5526 (0.5%) of lung cancers [21/5172 (0.4%) of non-small cell lung carcinoma (NSCLC) and 6/354 (1.7%) of small cell lung carcinoma] were MSI-H and/or MMR-deficient (MMR-D). The median age was 70 years, 48% were female, and 92% had a smoking history. The median tumor mutation burden was 32 mut/Mb (range: 15.7-62 mut/Mb), and 7/18 (39%) expressed PD-L1. Notably, 59% had a somatic *MLH1* alteration [truncating mutations (n=6), splice site mutations (n=5), homozygous deletions (n=2), and promoter hypermethylation (n=2)]. All tested cases with *MLH1* alterations had loss of MLH1 and PMS2 expression by IHC. Others had somatic *MSH2* (7%) and *MSH6* (7%) alterations, leaving 26% without somatic MMR alterations. The overall prevalence of MSI-H/MMR-D cases in this cohort mirrored the results in the NSCLC TGCA dataset (6/1002, 0.6%) and with similar clinical and molecular features (prominent smoking history and recurrent *MLH1* mutations with reduced MLH1 mRNA expression). In our cohort, 3/9 patients treated with immune checkpoint inhibitors experienced durable clinical benefit.

Conclusions: Genuine MSI is present in a small subset of lung cancers that are associated with smoking and somatic *MLH1* inactivation.

952   Correlation of Histologic Features with Gene Alterations in Malignant Pleural Mesothelioma

Soo-Ryum Yang[1], Meier Hsu[1], Kay See Tan[1], Prasad Adusumilli[1], Jason Chang[1], Michael Offin[1], Natasha Rekhtman[1], William Travis[1], Marjorie Zauderer[1], Marc Ladanyi[1], Jennifer Sauter[1]
[1]Memorial Sloan Kettering Cancer Center, New York, NY

Disclosures: Soo-Ryum Yang: None; Meier Hsu: None; Kay See Tan: None; Prasad Adusumilli: None; Jason Chang: None; Michael Offin: None; Natasha Rekhtman: None; William Travis: None; Marjorie Zauderer: None; Marc Ladanyi: None; Jennifer Sauter: None

Background: Histologic features including nuclear grade, architectural patterns and presence of necrosis have been shown to have prognostic significance in epithelioid (E) malignant pleural mesothelioma (MPM). Correlation of these features with gene alterations has not been reported.

Design: All available MPM specimens with next generation sequencing (NGS) data at study institution were retrospectively reviewed to assess for presence of necrosis and histologic subtype: (E), biphasic (B) and sarcomatoid (S). E MPM were further assessed for nuclear grade (3-tier derived from atypia and mitotic scores, as previously published) and architectural patterns: Tubulopapillary (TP), trabecular (T), micropapillary (MP), solid (Sd) and pleomorphic (PL), including predominant as well as presence of any pattern. Correlations of histologic features with gene alterations overall, and within the subset of E MPM only, were assessed by Fisher's exact tests.

Results: 182 patients (median age 70 years, 76% male) with MPM (129 (71%) E, 47 (26%) B and 6 (3%) S) and NGS data available were identified. E MPM showed highest rate of *BAP1* alterations (68%), whereas *CDKN2A* (55%), *NF2* (53%) and *LATS2* (19%) were frequent in non-E tumors (Table 1). Compared to wild type, *TP53* and *LATS2* mutations were associated with necrosis (17/29 (59%) vs. 38/153 (25%), p<0.001 and 12/20 (60%) vs. 43/162 (27%), p=0.004, respectively), while necrosis was uncommon in *SETD2*-altered MPM (2/22 (9%) vs. 53/160 (33%), p=0.004). Distribution of necrosis among molecular subsets was similar in E MPM. Most common predominant architectural pattern in E MPM (n=129) was Sd (50%), followed by TP (25%), T (16%), PL (7%) and MP (2%). All *LATS2* (100% vs. 68%, p=0.03) and majority of *CDKNA2A*-altered E MPM had a least focal Sd pattern (84% vs. 63%, p=0.015). PL features were common in *LATS2*-altered E MPM (60% vs. 20%, p=0.01). *TP53*, *LATS2* and *CDKN2A* alterations were associated with higher nuclear grade (Table 1).

Gene alteration	All cases (n=182)				Epithelioid only (n=129)			
	All	Histologic subtype		p-value	Nuclear grade			p-value
	(n=182)	Epithelioid	Non-Epithelioid		I	II	III	
		(n = 129)	(n = 53)		(n = 9)	(n = 60)	(n = 60)	
BAP1	111 (61%)	88 (68%)	23 (43%)	**0.003**	6 (67%)	44 (73%)	38 (63%)	0.5
CDKN2A	74 (41%)	45 (35%)	29 (55%)	**0.02**	0 (0%)	18 (30%)	27 (45%)	**0.014**
NF2	56 (31%)	28 (22%)	28 (53%)	**<0.001**	1 (11%)	10 (17%)	17 (28%)	0.3
TP53	29 (16%)	17 (13%)	12 (23%)	0.12	0 (0%)	4 (6.7%)	13 (22%)	**0.041**
SETD2	22 (12%)	16 (12%)	6 (11%)	>0.9	2 (22%)	9 (15%)	5 (8.3%)	0.3
LATS2	20 (11%)	10 (7.8%)	10 (19%)	**0.038**	0 (0%)	1 (1.7%)	9 (15%)	**0.027**
PBRM1	15 (8.2%)	13 (10%)	2 (3.8%)	0.2	0 (0%)	7 (12%)	6 (10%)	>0.9

Conclusions: E MPM with *LATS2*, *CDKN2A* and *TP53* alterations were enriched in poor prognostic histologic features including high grade, necrosis and Sd pattern. At least focal PL features were common in *LATS2*-altered tumors. These observations warrant future study in larger cohorts.